Bachelor's project

NTNU
Norwegian University of Science and Technology
Faculty of Engineering
Department of Manufacturing and Civil Engineering

Marius Bredesen
Edwin Helder

Analysis of the positional accuracy of a low-cost dual frequency GNSS-module

The capabilities of the u-blox ZED-F9P

Bachelor's project in Geomatics
Supervisor: Vilma Zubinaite
May 2019

NTNU
Kunnskap for en bedre verden

Marius Bredesen
Edwin Helder

Analysis of the positional accuracy of a low-cost dual frequency GNSS-module

The capabilities of the u-blox ZED-F9P

Bachelor's project in Geomatics
Supervisor: Vilma Zubinaite
May 2019

Norwegian University of Science and Technology
Faculty of Engineering
Department of Manufacturing and Civil Engineering

NTNU
Norwegian University of
Science and Technology

NTNU
Institutt for vareproduksjon
og byggteknikk

Title of the thesis:	Date: 19.05.19			
Analysis of the positional accuracy of a low-cost dual frequency GNSS-module	Number of pages: 110			
	Masterthesis:		Bachelorthesis	x
Name: Edwin Helder Marius Bredesen				
Supervisor: Vilma Zubinaite				
External supervisors: none				

Summary:

The purpose of our thesis is to test the new GNSS module, ZED-F9P released by u-blox. In order to do this, we analyze the measurements to see which applications the module is best suited for. The measurement methods we choose to use for the analysis, are different types of real-time measurements, as well as different types of phase-based static measurements. The real-time measurements consist of dynamic and stationary (static) measurements, as well as the accuracy we can expect.

The static measurements consist of measuring periods of 1,3,6 and 24 hours, logged on three pillars with different surroundings. These measurement periods are later compared, in order to see how high accuracy that can be achieved with the different time intervals. Afterwards the results are compared with corresponding measurements made by a Leica GS16 receiver. The adjusted coordinates from the 24-hour measurements are considered as the coordinates closest to the absolute position of the pillars. These coordinates then form the basis for our analysis of u-blox module measurements.

The results from all the static measurement periods were surprisingly good, the u-blox measurements had somewhat larger standard deviation but managed to keep up with Leica. All measurements had a maximum difference of 1.27cm in S1, which was from the u-blox 1-hour measurement to the u-blox 3-hour measurement. Real-time measurements with u-blox also provided the expected accuracy of 1-3cm, but in two datasets, systematic errors occurred, as a result of our antenna being affected by multipath.

As a conclusion, static measurements with post-processing provide expected accuracy, and the differences between F9P and GS16 are not in the receiver itself. But the real-time measurements show that the antenna we bought for 400 NOK is not very resistant to multipath. On the other hand, a high-quality antenna may provide more consistent accuracy for real-time measurements.

Key Words:

ZED-F9P, RTK, static, dynamic
RTKLIB , Infinity , GFZRNX
Precision
Accuracy

Edwin Helder Marius Bredesen

Abstract (Norwegian)

Formålet med vår oppgave er å teste den nye GNSS-modulen, ZED-F9P utgitt av u-blox. For deretter å analysere målingene for å se hvilke bruksområder modulen er best egnet til. Målemetodene vi velger å bruke til analysen er forskjellige typer sanntidsmålinger, samt forskjellige typer fase-baserte statiske målinger. Sanntidsmålingene består av dynamiske og stasjonære målinger, samt hvilken nøyaktighet vi kan forvente av disse.

De statiske målingene består av måleperioder på 1,3,6 og 24 timer, logget på tre forskjellige søyler med forskjellige forutsetninger for satellitt dekning. Disse måleperiodene skal da sammenliknes for å se hvor høy nøyaktighet man kan oppnå med de forskjellige måle-tidene, samt at resultatene sammenliknes med tilsvarende målinger gjort av en Leica GS16 mottaker. De utjevnede koordinatene fra 24-timers målingene antas å være det resultatet som gir koordinater nærmest den absolutte posisjonen til søylene. Disse koordinatene utgjør da grunnlaget for vår analyse av målinger med u-blox-modulen.

Resultatene fra alle de statiske måleperiodene ble overaskende gode, u-blox målingene hadde noe større standardavvik, men klarte å holde følge med Leica. Alle målinger hadde en maksimal spredning på 1,27cm i S1, som var fra u-blox 1-times målingen, til u-blox 3-times målingen. Sanntidsmålingene med u-blox ga også forventet nøyaktighet på 1-3cm, men i ett par av målingene oppstod det systematiske feil som en følge av at antennen vår muligens ble påvirket av flerveisinterferens.

Man kan konkludere med at statiske målinger med etter-prosessering gir forventet nøyaktighet, og at forskjellene mellom F9P og GS16 ikke ligger i selve mottakeren. Men sanntidsmålingene viser at antennen vi kjøpte for 400 NOK, ikke er veldig resistent mot flerveisinterferens. En antenne av bedre kvalitet kan muligens gi mer konsise sanntidsmålinger.

Forord

Bacheloroppgaven er vårt siste steg ut av studenttilværelsen inn i fremtiden.

En stor takk til vår veileder, Vilma Zubinaite. Vi har satt stor pris på all veiledning og hjelp i arbeidet med denne oppgaven og for å holde oss på rett spor.

Vi vil også rette en takk til alle andre ved NTNU, Leica Geosystems og Statens Kartverk, som har bidratt med utstyr og forskjellige innspill under arbeidet med oppgaven.

Og ikke minst, et stort takk til familiene våre for støtte, og for å tåle mitt fravær (Edwin) det siste året.

Og et spesielt takk til Desiré Trinborg for illustrasjoner og grundig korrekturlesing.

And a thanks to Franklin2 at GitHub, who provided us with several updates of RTKLIB-binaries, and without whom we would not have been able to do some of our testing.

Marius Bredesen, Edwin Helder

Gjøvik, 19. mai 2019.

Table of contents

Table of figures

Table of tables

1 Introduction

The last 10- 15 years Global Navigation Services, based on satellites, have started to play an important role in everyday lives. GPS's, car navigation, mobile phones, and also many behind-the-scene applications. With the increasing use of positioning services, the demand for higher accuracy also increased; autonomous cars, surveying equipment and mobile phones, but also monitoring of for example geological phenomenon. Equipment with high accuracy has mainly been restricted to governments and professional users like land surveyors, due to the high prices for the equipment.

In June 2018, Erik Oppedal wrote his master thesis about "Analysis of positional data from GNSS-receivers on vehicles". Oppedal's purpose was to analyze the accuracy of present code based GNSS receivers when mounted on a car and by using a carrier phase receiver as a reference. In the abstract he writes the following (Oppedal, 2018)

> Code-based GNSS receivers can be the future of automotive navigation systems as they can offer accurate and robust GNSS measurements at a low cost. If GNSS receivers can achieve accuracy to determine the lane of a vehicle, they can become an important part of future automotive navigation systems supporting autonomous vehicles.

Oppedal then comments on the results of code based GNSS receivers (Oppedal, 2018):

> The results documented a positioning accuracy of approximately 1.3 m, given by the root mean square of the positioning errors, which was better than expected based on the data sheets. The measured accuracy is not adequate for «lane-level positioning» and indicate that there is still need for improvement in order to use code-based navigation units to achieve the goal of autonomous vehicles.

He then makes a conclusion that dual-frequency antennas with differential phase measurements could be the solution, but cost is an issue (Oppedal, 2018, own translation):

> The coordinate accuracy from dual frequency-antennas performing differential phase measurements in real time are good enough to achieve these goals. The problem is that the price level for multi frequent receivers is high. In 2013 the price was ca. 100.000 NOK (Skogseth and Norberg, 2014), and in 2018 the prices are still high. If cars would be equipped with such receivers, this would have made up a reasonable part of the total production costs and that would be totally unacceptable. While driving there are in addition challenges with the use of phase measurements because of frequent interruptions meanwhile have code measurements shown to be more robust and can give good positions for a bigger part of the route

The Galileo-organization has also done research on this topic: "*For fully autonomous driving to become reality, several technologies will have to reach maturity and be rolled out in concert. One of them is affordable, scalable, and reliable high precision positioning."* (Galileognss.eu, 2018)

It shows that positioning accuracy at centimeter or even millimeter level, was only achievable by professionals with professional GNSS equipment with a big price tag. There have been some GNSS-modules available in the medium price range the last years. With the introduction of the ZED-F9P module from u-blox, which is a dual-frequency GNSS receiver said to be capable of position-accuracy comparable with professional equipment, positioning with high accuracy should be available at a much more reasonable price. Our tested eval board based on the ZED-F9P goes for a retail price of about $ 250.

With our interest in software, hardware and the idea of a "do it yourself" GNSS rover setup, there was no doubt that we wanted to test and analyze to see what this module was capable of, compared to professional GNSS-receivers, and if this even might replace more expensive equipment in certain use-cases.

We planned to test the ZED-F9P with three different methods, that could give us an idea of the capabilities of the module under different conditions, and if the module lives up to the accuracy promised by the manufacturer.

The first method was to test the module under static conditions where the module is placed on a benchmark for a predefined time period where its position is logged every second. With the goal to get an insight in the accuracy which can be obtained with the module and what time period would be enough to reach sufficiently accuracy for land surveying. In this part we also wanted to compare the ZED-F9P with a professional rover; the Leica GS16 in order to see if there would be clear differences in accuracy and eventually precision between the ZED-F9P and the Leica GS16.

The second method was to test the module with real time kinematic measurements. With the use of real time kinematic, it is possible to establish the coordinates of an unknown point in real time with an expected accuracy of up 1-3 cm (Tersus-gnss.com, 2019). The module would still be mounted static on a benchmark. The goal of this method was to test the ability to obtain fix-status, which is necessary to be able to establish the coordinates of an unknown

point in real time and the accuracy which can be achieved with the module. This method was going to be based on series of 10 conclusive measurements with a 2 second cycle, which would give an insight in the precision which can be achieved with the module. The static measurements were done on benchmarks located at the NTNU in Gjøvik (Norway).

The third method was to test the module in dynamic mode. In dynamic mode, the module is in movement where its position is was re-established every five seconds. The aim of this method was to test the ability to keep and eventually retain fix-status under dynamic conditions. This is technically the most demanding method and it would also give an idea of the possible accuracy under changing conditions. The dynamic measurements were done at a minor road in Østfold (Norway).

Since the ZED-F9P was going to be used with open source software, it would need to be completed with an antenna and controller in order to make it a functional GNSS-receiver. Testing the capabilities of these parts would also be a part of the project. We built two similar setups to increase the possibility to eliminate accidental production errors in the equipment, by being able to compare both conclusive and simultaneous measurements.

With these three methods in mind, we also want to give some ideas about possible uses for the ZED-F9P and some recommendations for other tests.

2 Theory

2.1 History of Global Navigation Satellite Systems

Already during World War II, the USA among other countries, built a long-distance navigation system called LORAN (Long Range Navigation). The system was based on a chain of multiple radio beacons, with a master and slave stations, broadcasting on low frequencies with long wavelengths. The master station sends a pulse signal that is received by one or more slave stations. When receiving the signal from the master, the slave sends its own pulse with a known delay based on the known distance between the beacons. The time difference between the master and slave pulse signal makes it possible to calculate the relative distance from receiver to both the master and slave stations. There is still a wide range of points along a hyperbole where this is true, but by combining signals the possible location is narrowed down to two intersections of the hyperboles where one easily can be ruled out. (Forssell, 2019)

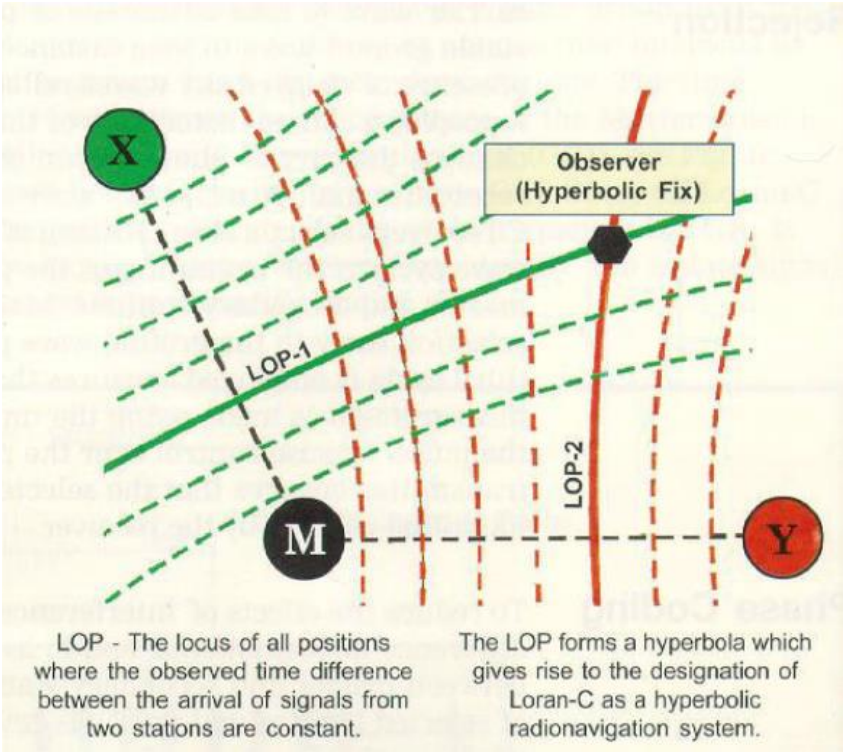

Figure 1 - Crossing Locus of Positions show the position of the observer (Coast Guard Aviation Association, 2019)

The basic theory behind this way of navigating is called trilateration. The LORAN system went through many minor and major changes and by the time it was fully matured in the sixties the technology forming the foundation of the upcoming GPS-system was in place.

By then, the US Department of Defense already ordered the development of a satellite-based navigation system.

2.1.1 How does Global Satellite Navigation work?

Satellite navigation systems are built around satellites orbiting in known trajectories around the earth. The satellites are broadcasting their signals continuously, those signals can be tracked by GNSS receivers. Those receivers are often referred to as GPS by regular people, because USA's Global Positioning System (GPS) was the first satellite navigation system. By now there are four different constellations with global coverage and a better word would be GNSS-receiver; from Global Navigation Satellite System. A satellite navigation system consists of a control segment, a space segment and a user segment. The control segment monitors the satellites and stands for the maintenance of both hardware and software of the satellites. The space segment is made up of the satellites. The user segment is the different users; governments, compagnies, private persons and land surveyors.

To make it possible for a GNSS-receiver to find its position it needs signals from at least four different satellites. The mathematics behind this is complex but is based on that there are four unknown values which need to be calculated. The receiver's position in three directions X, Y and Z and the fourth is time. To enable the receiver to have free sight to at least four satellites from almost all places on earth the different GNSS-systems have from 24 to over 30 satellites.

Like its predecessor LORAN, satellite navigation is based on what is called trilateration. Trilateration is the principle that the observer or receiver can calculate its position (here in a plane) when knowing the distance to three points with a known position. (Circuit Cellar, 2014)

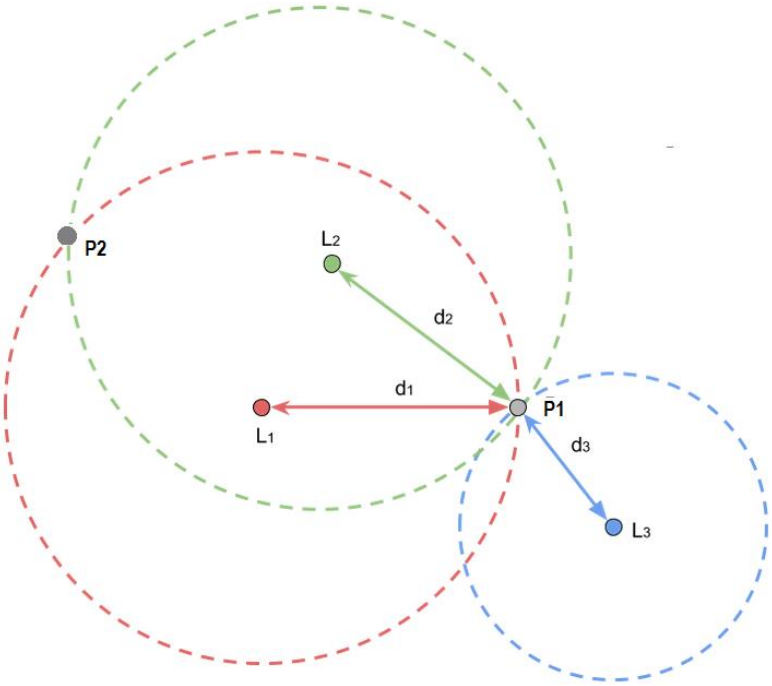

Figure 2 - The principle of trilateration (Zucconi, 2017)

When the position of L1, L2 and L3 are known, circles with a radius of the known distances d1, d2 and d3, can be drawn. The circles will then meet in one point, point P1, which is the position of the observer.

Calculating the distance to a known point, is based on the time delay between when a signal is sent and when the signal is received. Radio signals travel with the speed of light, 299 792 458 m/s (Skaar and Linder, 2019). When measuring time delay over shorter distances, microseconds are no longer enough for achieving "high" accuracy. Light travels approximately 300 m in one microsecond and 30 cm in one nanosecond. First in 1955, atomic clocks that could measure time with an accuracy of nanoseconds were built. The commercial scale production of semiconductors at the same time together with Russia launching the first artificial satellite Sputnik 1 in 1957, were the last pieces falling in place for building a global positioning system (Circuit Cellar, 2014). American scientists quickly realized that measuring the doppler effect on the beep transmitted by the Sputnik 1, enabled them to calculate the position of the satellite. This became the fundamentals of satellite-based positioning.

In order to calculate the time delay, it is required to know when the signal was sent by the transmitter, and when it was received by the receiver. Satellites add a time stamp to their

signal to let the receivers know when the signal left the satellite. To enable the receiver to calculate a time delay, it is also required that the receiver's clock is synchronized with the satellite clocks. In addition to the time stamp, the satellites also modulate a code on the carrier wave of the radio signal. The code is called the coarse acquisition code or pseudo-random code. The code has a length of 1023 elements or chips, broadcasted at a rate of 1.023 Mhz. This means that the code repeats itself every millisecond. The length of the signal is the same as the distance light travels in one millisecond, about 300 km. The length of a chip is 300 km divided by 1023, 293 meters.

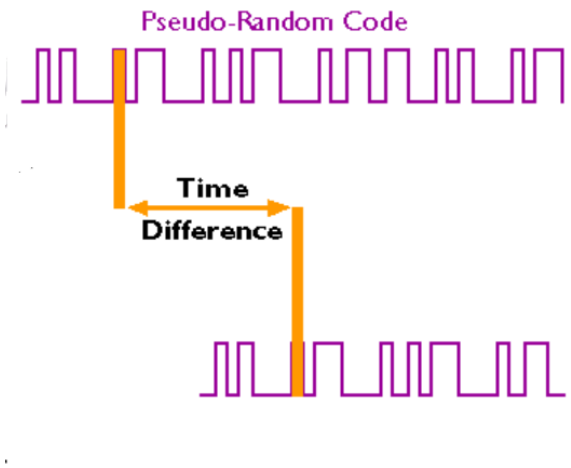

Figure 3 - time difference measured in the pseudo-random code (Bhatti, 2019)

Every satellite is broadcasting its own unique code and the receivers have a copy of all the codes. By comparing the codes from different satellites with the internal codes, the receiver can identify the satellites and calculate the time difference, shown in *Figure 3*. Since the receiver also is aware of when the signal was transmitted through the time stamps, the receiver can now calculate the distances to the satellites. The accuracy from the chip is defined by its length, approximately 293 meters. Since modern receivers can track within the length of a chip, the accuracy is much higher than 293 meters. Depending on the circumstances, 5-10 meters. This is not accurate enough for surveying purposes. Together with the coarse acquisition code, satellites also broadcast more precise codes as the P-code for GPS. The more precise codes, often referred to as military codes, are not available for civilian use. The precise codes are broadcasted on another frequency. This combined with a higher chip rate of 10.23 Mhz, provides an accuracy of about 2-5 meters.

Even military codes are not accurate enough for surveying purposes. Already during WW II scientists experimenting with LORAN realized they could use the wavelength of the carrier

wave of a radio signal, in order to determine the distance to the transmitter. Radio signals behave as waves with peaks and troughs.

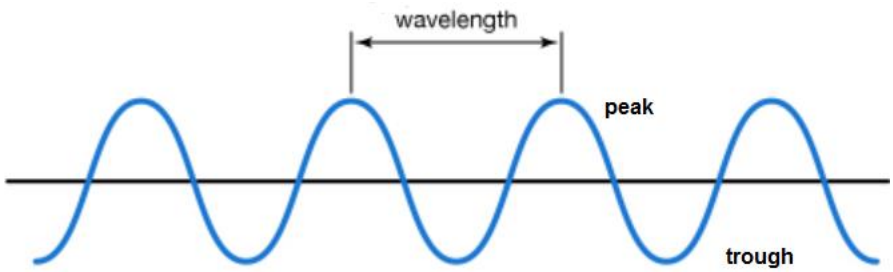

Figure 4 - radio signal and its wavelength (Encyclopædia Britannica Inc., 2019)

The wavelength is the distance between two following peaks or troughs. The higher the frequency of the signal, the shorter the wavelength. Satellites broadcast their signals on frequencies ranging from ~1.2 to 1.6 GHZ, and wavelengths ranging from ~19 to 25 cm. By counting the number of complete wavelengths and multiplying this with the length of the wave, it becomes possible to calculate the distance between the transmitter and the receiver. The challenge is to know the number of wavelengths between satellite and receiver; the integer ambiguity of the signal. The number of wavelengths can in theory be anything between one and infinite. In practice this is bound to limits within the range between the possible locations of the satellites and roughly the earth's surface. With a wavelength of 19 to 25 cm this is still a high number.

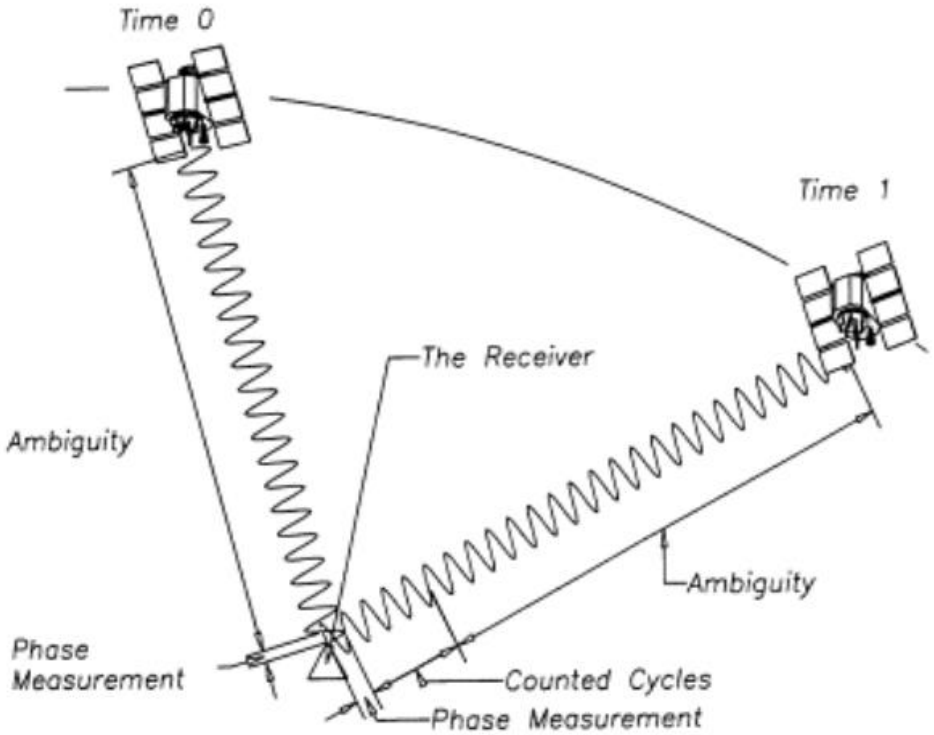

Figure 5 – Carrier phase-based measurements (Nptel.ac.in, 2019)

However, the approximate distance between the satellite and the receiver is already known from the pseudo-range, with an accuracy of a few meters. By using the pseudo-range, the number of possible candidates or solutions for the ambiguities can be reduced to a number that can be handled by the receiver; four to five wavelengths for every meter. When the receiver has solved or calculated the number of wavelengths for enough satellites, this is called fix or fix-status. Once the receiver knows the number of wavelengths between the satellite and itself it can keep track in the change of position of the satellite. The receiver needs at least four satellites to find its position and reach the fix-status, but more satellites generally gives higher accuracy, due to the possibility for the receiver to check measurements in solution for errors against other measurements for possible.

Positioning with satellites is sensitive for errors. Some of the errors are connected to the receiver side, others are connected to the satellite and some are connected to what is happening in between with the signal. Receiver side errors are internal delay or noise in the receiver, clock drift and uncertainty about the exact central point of the antenna. This is called the phase center. These errors range from 1-5 millimeters for the phase center, to up to 20-30

centimeters for receiver noise. Another error connected to the receiver is a phenomenon called multipath. This happens when the signal from the satellite reflects of an object before reaching the receivers antenna. Although this is an error occurring between satellite and receiver, it only occurs locally resulting in errors up to about 1 meter.

Besides being disturbed locally, there is another source of possible errors which will work over bigger areas. Radio signals travel at 299 792 458 m/s in vacuum but will be slowed down on their way through the atmosphere. The relative permittivity for the air is not much higher than for vacuum, but this error might be in the range of 5-6 meters.

As with the receiver, the satellites might suffer from clock drift. Satellite clocks are precise, but with a speed of light of ~300.000 km/s an error of 4-6 nanoseconds lead to errors of 1-2 meters. The orbits of the satellites are defined and maintained by the control segment. But just like the sun and the moon cause the tides because of their gravitational force on water they will also slightly affect the orbits of satellites. For navigational satellites this might lead to errors up to 2-3 meters.

Errors affecting the signals, such as the clocks and the orbits are usually called systematic errors, due to having approximately the same deviation over bigger areas. This means that that will give errors of the same size for two or more different receivers spread over an area with radiuses from 15-30 km.

To minimize the effect of such systematic errors, a method called differential GNSS can be used. This method is based on the idea that when a receiver is placed in a point with a known position, one will measure coordinates which are affected by errors. By subtracting the known coordinates from the measured coordinates, it is possible to calculate the size and direction of the errors. The calculated values for errors can be used to correct coordinates measured with other receivers in unknown points.

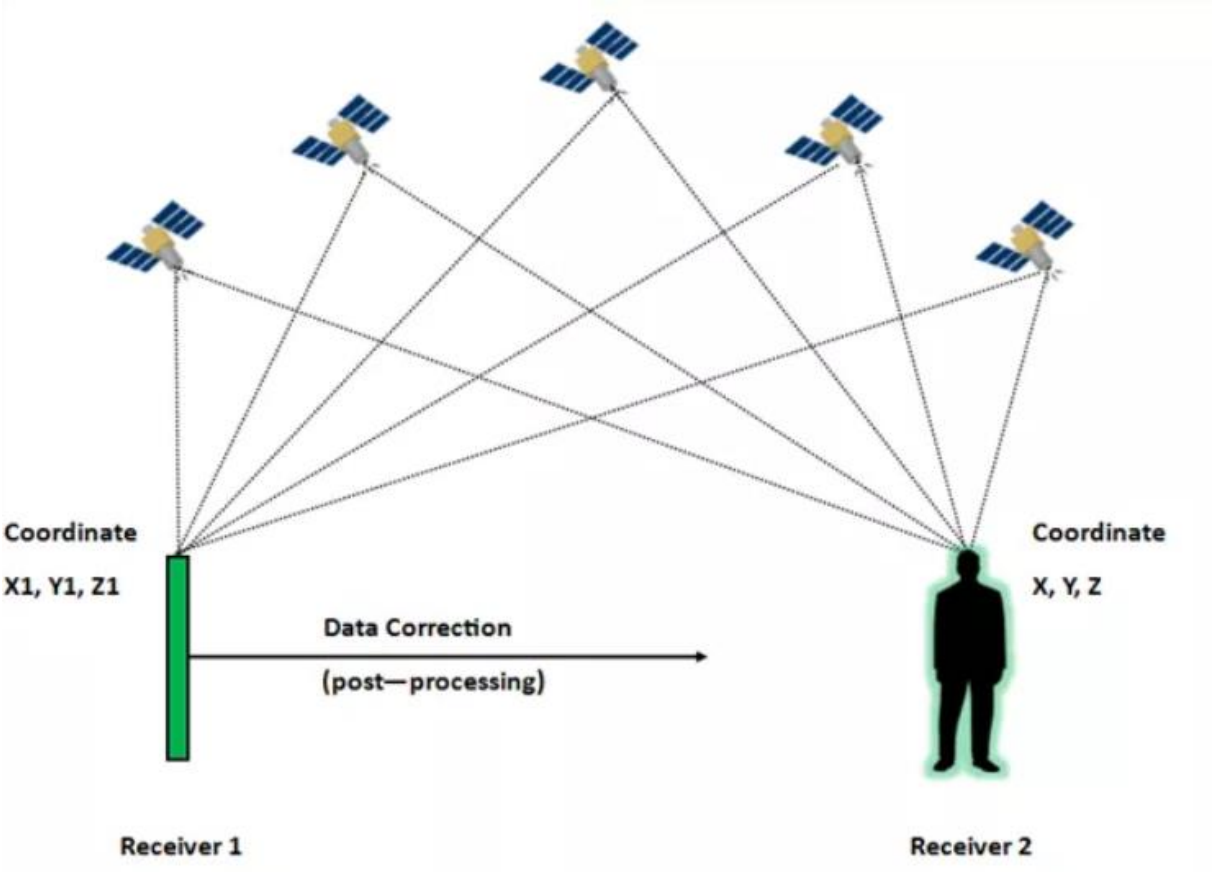

Figure 6 - The basic concept of differential GNSS. (Difference Between GPS and DGPS, 2019)

The receivers should be within a range of 30 to 50 kilometer and a prerequisite is that both receivers use the same satellites. The virtual line between base and rover is called baseline or baseline vector.

This correction data can be sent from one receiver by radio link or internet, to another receiver. This is called real time kinematic measurements, where the receiver with known coordinates is called base or reference station and the other is called rover; respectively receiver 1 and receiver 2 in *Figure 6*.

2.1.2 GPS - Global Positioning system

The satellite-based navigation system developed by the United States, was named NAVSTAR, which later was changed to GPS. The first GPS satellite was launched into space in 1978, and the system has been fully operational since 1995. The satellites were sent in an orbit that makes a 55-degree angle on the equator plane. (Forssell, 2019)

Today, the GPS satellite system contain 31 functional satellites, all of which is in medium earth orbit at about 20 000 km above the earth. This height is preferred since it allows satellites to do one lap around the earth in approximately 12 hours. All GPS satellites broadcast signals on L1 and L2 frequencies. Modern satellites also broadcast L1C, L2C as well as military codes. In order to work, the system rely on atomic clocks that are onboard every satellite. Those clocks are synchronized with each other, as well as the atomic clocks in the ground control segments. In addition to the clocks that provides accurate time, it is crucial that the current position of the satellites is known. Given this information, there is possible to calculate the receiver's position based on the constant speed of the radio waves transmitted. In order to achieve 3-dimentional position, the receiver must be in view of at least four satellites simultaneously. (Circuit Cellar, 2019)

GPS is designed to have coverage of at least four satellites at any given point on the globe, but surrounding terrain and other objects may block signals. Fortunately, there are several other satellite-systems that is also available for civilian use, that can help increase accuracy and coverage.

2.1.3 GLONASS

In 1982, another satellite-system started to form with the launch of the first satellites in the Russian system GLONASS. However, it wasn't until 1995 that all 24 satellites were operational. The Russian satellites is at a height of approximately 19 000 km, which is about 1000 km lower than GPS. GLONASS has an inclination angle on the equator plane at 64,8 degrees, this allow GLONASS to also have an orbit-time of about 12 hours (Forssell, 2019). All satellites in GLONASS is distributed in the orbit-plane in a way that gives evenly signal coverage on the ground. GPS on the other hand, have satellites uniformly distributed in the orbit-plane, which gives a more "random" signal coverage on the ground. *Figure 7* shows a data-sample for GLONASS.

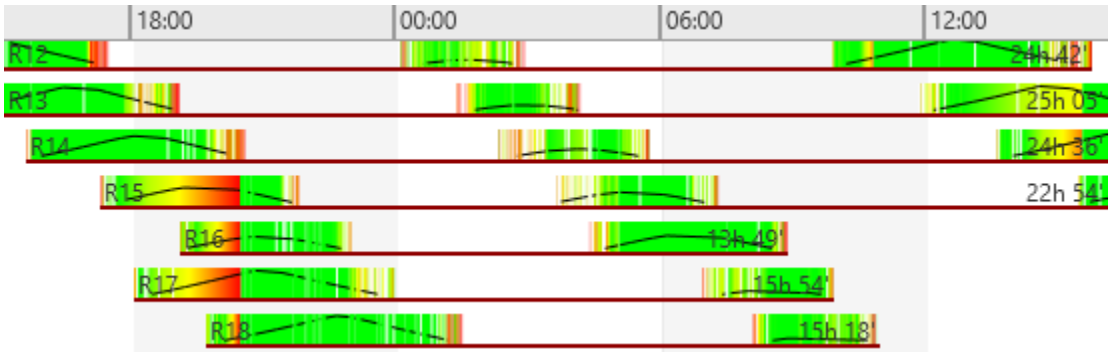

Figure 7 – Data-sample of GLONASS satellites

Not only can we see the evenly distributed satellites, we are also able to tell that one orbit takes about 12 hours. We received signals from R12 for the second time at midnight, and the next observation of that satellite is around mid-day, this proves the orbit time. In contrast, *Figure 8* shows data samples from GPS

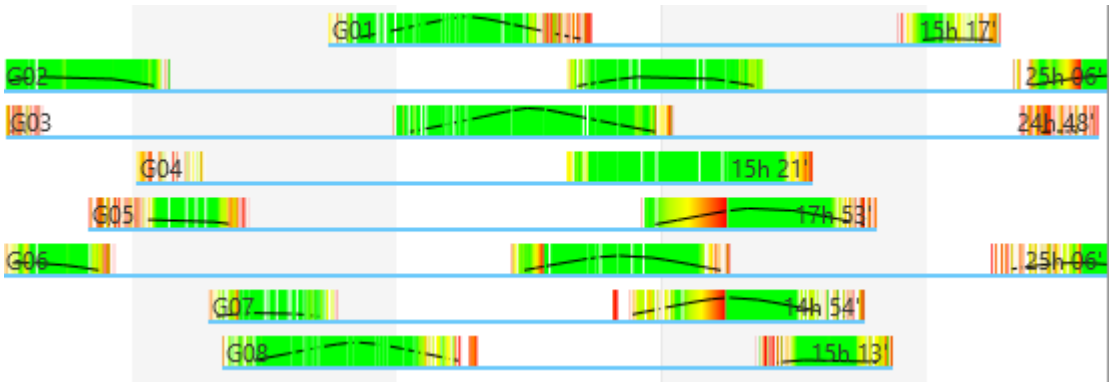

Figure 8 - Data-sample for GPS satellites

For GPS it is also possible to tell that the orbit-time is about 12 hours, but the satellite pattern is very different.

2.1.4 BeiDou

China launched the first satellite for its own navigation system in the year of 2000. In december 2018 it started to deliver global positioning services and is expected to be fully operational in 2020. BeiDou has a slightly different set up compared to the other three main navigation systems, which is that BeiDou combines both geostationary and medium earth orbit (MEO) satellites. The system is planned to consist of 5 geostationary satellites, 27 MEO satellites and 3 satellites with an inclined geosynchronous orbit. The MEO satellites has a slightly higher orbit than GPS satellites, resulting in a little less than two revolutions per day. (En.beidou.gov.cn, 2019)

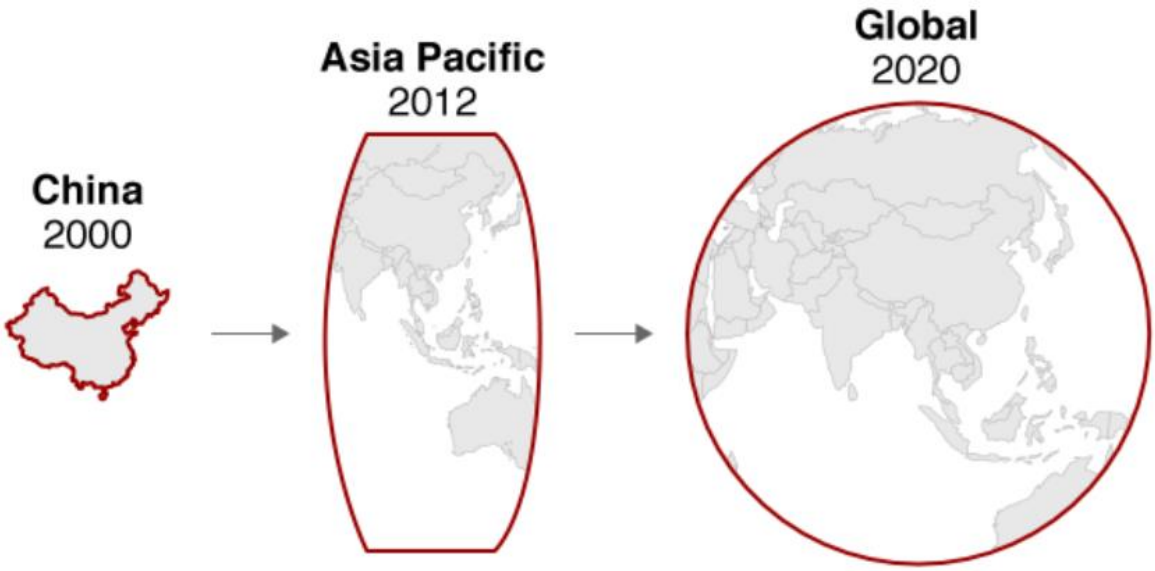

Figure 9 - The path from local to global navigation service: BeiDou (BBC News, 2018)

For GLONASS and Galileo, an important factor in developing their own satellite navigation system, was to be independent of GPS. For a period of five years from 2003, China was involved in the European Galileo-project. While simultaneously with building its own system. Unsatisfied with the cooperation with Europe, China started to focus on completing its own global service.

Although BeiDou is close to being fully operational, there is still lacking full coverage for Norway. This can easily be observed whilst looking at *Figure 10*

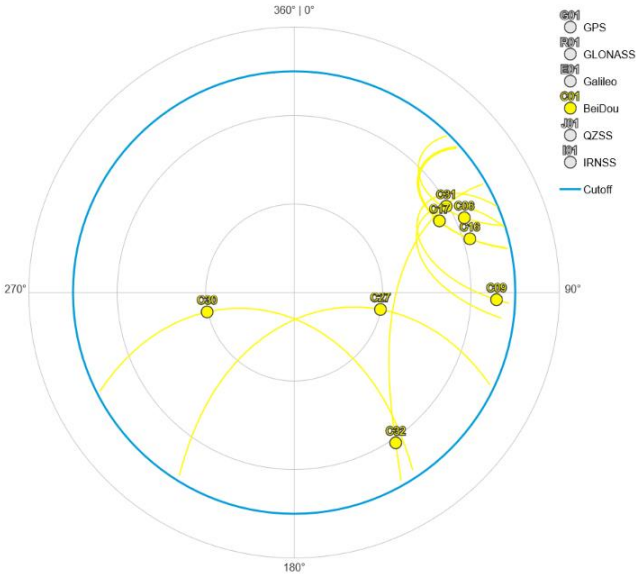

Figure 10 - Skyplot for BeiDou 11th of March 2019 22:00 UTC

Figure 10 shows that there are eight satellites visible, since being concentrated to the east, it is resulting in poor geometry. The effect of the poor geometry is seen in the DOP-values, with a spike at 22:00 which can be seen in *Figure 11*. The impact of DOP values will be discussed further in the thesis.

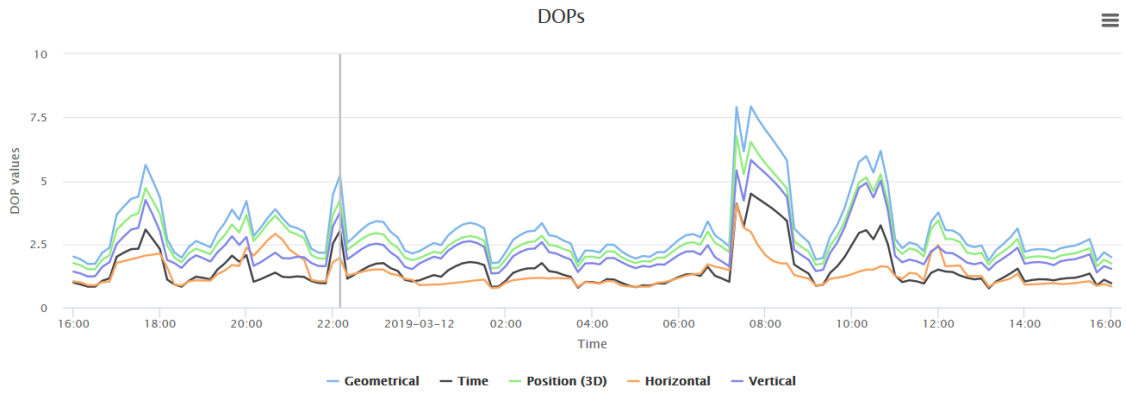

Figure 11 - DOP-values for only BeiDou 11th of March 2019 (18:00-18:00 UTC+1)

Figure 11 shows poor DOP-values for BeiDou, at a few given times of the day, which is a result of lacking satellite coverage.

2.1.5 Galileo

Galileo is the newest addition to global navigation satellite-systems, with their first launch in 2011. Galileo is the official GNSS made by the European Union, and the European Space Agency. The system is planned to be fully operational with 30 satellites in 2021, as a supplement to existing satellite systems, and as an independent satellite system.

Galileo is named after the Italian astronomer Galileo Galilei, which in year 1610 discovered four of Jupiter's moons. Like GPS and GLONASS, Galileo only has satellites in Medium Earth Orbit (MEO), slightly higher at an altitude of about 23 000 km. Opposed to the other systems, Galileo satellites transmit different frequencies referred to as E5a, E5b, E6 and E1. Measurements with Galileo as a standalone system, is proven to be more accurate than all other existing satellite systems. Where the main reason is better performing atomic clocks onboard the satellites. (Forssell, 2019)

2.1.6 Other

In addition to GPS, GLONASS, BeiDou and Galileo, there are a variety of other regional satellite systems. There is the Quasi-Zenith Satellite System (QZSS) which is a four-satellite regional time transfer system, as well as enhancements for GPS covering Japan. NAVIC or Navigation with Indian Constellation, is another regional system managed by the Indian Government consisting of 7 satellites, all located in geostationary and geosynchronous orbits. (En.wikipedia.org, 2019)

There are plenty of navigation satellites orbiting the earth, but in order to provide the accuracy and precision that is required in the positioning industry, the right hardware and software is required to be able to process the data provided by the satellites.

2.2 Static surveying measurements

Static GNSS measurements revolves around logging raw data transmitted by satellites, in a stationary point. The logging period is also referred to as occupation time. The occupation time refers to how long the rover should be kept static to achieve the desired level of accuracy. (Gssc.esa.int, 2019) In most cases where the static method is used, the desired level of absolute accuracy is quite high. Static measurements can be done by any GNSS receiver, but multi-frequency receivers are the only receivers that are able to achieve sub-centimeter accuracy paired with a capable antenna. Different governments worldwide are likely to have their own accuracy specifications to expect when measuring static. However, according to the *Norwegian Mapping Authority*, there is possible to achieve 2-4mm accuracy when using an occupation time of 24 hours. (Kartverket, p.10, 2009)

What makes static its own measuring-method, is the fact that you need to post-process the data gathered. The two most common ways to process the data, is by using surveying software to either apply final ephemeris and clock corrections, or to stick with broadcasted ephemeris and compute vectors between the points. The second option require reference stations which has a known position. In land surveying, vectors are the coordinate differences between two points.

2.2.1 Receiver Independent Exchange Format

Receiver Independent Exchange Format (RINEX), is the most commonly used data-format for GNSS observation and navigation data, due to it being a receiver brand independent. A version of RINEX is supported in most, if not all surveying software that is based around GNSS. RINEX is currently at version 3.04, which allowed the format to support the BeiDou satellite system that recently became available for global positioning in December 2018. With the addition of BeiDou, RINEX now supports all major constellations. (Igs.org, 2019)

2.3 Real-time kinematic measurements

A requirement for Real Time Kinematic is to get correction data which can be used by the receiver in order to calculate its position. These can be collected from three different sources. In Norway the most used non-commercial correction data source is CPOS. CPOS is based on a network of approximately 200 base stations with density of 35 to 70 km depending on the area. With a higher density in more populated areas, CPOS is owned by *Statens Kartverk* (Norwegian Mapping Authority) and is responsible for operating and maintaining the network. CPOS is non-commercial but requires a license to obtain login-parameters. Depending on the license, these can be used both to establish connection with the NTRIP-server and to download data for post-processing from ETPOS. When connecting to CPOS, CPOS creates a virtual reference station (VRS) based on the C/A-code from the satellites. This course acquisition provides a location which is close to the real position of the receiver. The VRS is based on 6 base stations closest to the receiver.

A second possibility is obtaining data from one base station to create a base line or several base stations in a network. This looks similar to CPOS but there are some differences. With a single base line or a network of multiple base lines there isn’t established a VRS and the correction data is streamed constant.

The SATREF-network (CPOS and ETPOS) can create such base lines but is usually only used for testing or special cases. Many commercial networks like Smartnet (Leica) and TopNET (Topcon), work in the same way. They might own their own base stations, but they might also be partially based on using data from governmental operated networks.

The third possibility is to set up one's own base station or stations. This can for example be done by local mapping authorities, but it might also be done by commercial actors. The base station might be permanent or temporary, the latter in a typical rover-base set up.

The accepted method of establishing new benchmarks with RTK, is based on the idea that the sets on the conclusive day is done with at least an hour offset to the previous ones. This is done with the idea that GPS repeats its cycle twice a day (23H 56M), and the hour offset will give measurements against different satellites which gives a different geometry. With the implementation of both Galileo and BeiDou (also into SATEF), the number of satellites has increased drastically, and it might be less relevant in future measure with an hour offset on conclusive days. The practice might get a revision in near future.

2.4 Precise Point Positioning

Precise Point Positioning is a technique that removes or models GNSS system errors in order to provide high levels of accuracy from a single receiver. A PPP solution depends on GNSS satellite clock and orbit corrections (NovAtel, 2014). These corrections are provided by the International GNSS Service (IGS), and there are different products. One of the commonly used products are Rapid ephemeris, this product is generated daily. Final ephemeris is the other commonly used product, final ephemeris provides the highest accuracy, but are only generated once a week every 12-18 days. Ephemeris are exact descriptions of the orbits of satellites or natural astronomical objects. Rapid ephemeris is often the preferred product, due to the accuracy gain between the two being miniscule (Igs.org, 2019):

Type		Accuracy	Latency	Updates	Sample Interval
Broadcast	orbits	~100 cm	real time	--	daily
	Sat. clocks	~5 ns RMS ~2.5 ns SDev			
Ultra-Rapid (predicted half)	orbits	~5 cm	real time	at 03, 09, 15, 21 UTC	15 min
	Sat. clocks	~3 ns RMS ~1.5 ns SDev			
Ultra-Rapid (observed half)	orbits	~3 cm	3 - 9 hours	at 03, 09, 15, 21 UTC	15 min
	Sat. clocks	~150 ps RMS ~50 ps SDev			
Rapid	orbits	~2.5 cm	17 - 41 hours	at 17 UTC daily	15 min
	Sat. & Stn. clocks	~75 ps RMS ~25 ps SDev			5 min
Final	orbits	~2.5 cm	12 - 18 days	every Thursday	15 min
	Sat. & Stn. clocks	~75 ps RMS ~20 ps SDev			Sat.: 30s Stn.: 5 min

Figure 12 - The different types of ephemeris (Igs.org, 2019)

2.5 Software

In this thesis, a range of different software are used. The reasoning behind being that we want to look at free software, as well as premium software. Some of the software has a limited purpose and is simply used to prepare data for another software.

2.5.1 Leica Infinity

Leica Infinity is a software designed to be used as an all-in-one program for land-surveying, including everything from TPS measurements, GNSS measurements, Level measurements BIM models, CAD, GIS and even GNSS post processing, that was previously only available in Leica Geo Office. The Leica geosystems webpage states the following features (Leica Infinity brochure, 2019):

- Import, visualize, and manage data easily, all in the 3D viewer
- Prepare survey or infrastructure data including roads, surfaces and control points for field crews
- Generate and save reports in your project for complete traceability
- Process Terrestrial TPS & Level data and Triple frequency multi constellation GNSS data
- Full 3D, 2D, 1D Network Adjustments to produce reliable control coordinates
- Use and manage images from the field including measuring points from images
- Work with scan point data including full 3D meshing tools
- Field to Finish for efficient CAD deliverables
- Leica SmartNet integration for downloading GNSS reference data
- Complete spatial awareness with HxIP imagery and default base maps
- Use the Leica Exchange, Leica ConX data services for efficient data transfer

2.5.2 GISline Oppmåling

GISline Oppmåling, developed by Norkart AS, is a software widely used among Norwegian local authorities, to easily follow national standards for land-surveying documentation. It is also a reliable tool for data collection, editing, processing and reliability analysis (Norkart, 2019). We used GISline in order to visualize the different types of measurements, with the help of WMS maps.

2.5.3 GFZRNX

GFZRNX is a software used to handle RINEX-files. It is developed by Thomas Nischan at GFZ German Research Centre for Geosciences in 2016. It supports observation, navigation and metrological data from most satellite systems and is available for most pc platforms. There is no GUI, which makes it a lightweight software. *Statens Kartverk* use the software when creating the headers of their RINEX-files. We used this to convert between RINEX versions. (Nischan, 2019)

2.5.4 RTKLIB

RTKLIB was developed in 2006 by Tomoji Takasu and Akio Yasuda at the Laboratory of Satellite Navigation, Tokyo University of Marine Science and Technology. It started out as an internal program for testing with GPS but from 2009 it was distributed as open source and available for external update and continuing development. The same year support for NTRIP, RTCM and multiple receivers was added together with the incorporation of GLONASS as second constellation. Today RTKLIB runs on Windows, Android or LINUX-platforms and supports the following features: (rtklib.com, 2007)

> (1) It supports standard and precise positioning algorithms with:
>
> GPS, GLONASS, Galileo, QZSS, BeiDou and SBAS
>
> (2) It supports various positioning modes with GNSS for both real-time and post-processing:
>
> Single, DGPS/DGNSS, Kinematic, Static, Moving-Baseline, Fixed, PPP-Kinematic, PPP-Static and PPP-Fixed
>
> (3) It supports many standard formats and protocols for GNSS:
>
> RINEX 2.10, 2.11, 2.12 OBS/NAV/GNAV/HNAV/LNAV/QNAV, RINEX 3.00, 3.01, 3.02 OBS/NAV, RINEX 3.02 CLK, RTCM ver.2.3, RTCM ver.3.1 (with amendment 1-5), ver.3.2, BINEX, NTRIP 1.0, RTCA/DO-229C, NMEA 0183, SP3-c, ANTEX 1.4, IONEX 1.0, NGS PCV and EMS 2.0 (refer the Manual for details)

(4) It supports several GNSS receivers' proprietary messages:

NovAtel: OEM4/V/6, OEM3, OEMStar, Superstar II, Hemisphere: Eclipse, Crescent, u-blox: LEA-4T/5T/6T, SkyTraq: S1315F, JAVAD: GRIL/GREIS, Furuno: GW-10 II/III and NVS NV08C BINR (refer the Manual for details)

(6) It supports external communication via:

Serial, TCP/IP, NTRIP, local log file (record and playback) and FTP/HTTP (automatic download)

(7) It provides many library functions and APIs for GNSS data processing:

Satellite and navigation system functions, matrix and vector functions, time and string functions, coordinates transformation, input and output functions, debug trace functions, platform dependent functions, positioning models, atmosphere models, antenna models, earth tides models, geoid models, datum transformation, RINEX functions, ephemeris and clock functions, precise ephemeris and clock functions, receiver raw data functions, RTCM functions, solution functions, Google Earth KML converter, SBAS functions, options functions, stream data input and output functions, integer ambiguity resolution, standard positioning, precise positioning, post-processing positioning, stream server functions, RTK server functions, downloader functions.

2.5.5 U-Center

U-center is a GNSS evaluation software developed by u-blox. Any receiver manufactured by u-blox is compatible with this software, and it is available for Windows and Mac. It is also used to update u-blox firmware, as well as configuring GNSS receiver modules. The official u-blox product summary states the following features: (Product Summary U-center, 2019)

- Support for NMEA and u-blox UBX binary protocol.
- Integrated AssistNow A-GNSS client functionality.
- Structured and graphical data visualization in realtime: Satellite summary view, navigation summary view, compass, speedometer, clock, altimeter, chart view of any two parameters of choice, data recording and playback functionality.
- Docking views (real-time cockpit instruments): Satellite constellation, compass, clock, altimeter, speedometer, GNSS and satellite information views.
- Full cut-and-paste functionality to transfer information to standard PC application software.
- Firmware update feature for u-blox receivers.
- RTCM protocol and NTRIP support.
- Map views, Google Earth server support, deviation map.

2.6 Services

2.6.1 CPOS - Centimeter Position

Centimeter Position, which is mostly referred to as CPOS, is a service that allows GNSS users to receive data over the internet, which improves the user's current position. As the name would imply, it can provide centimeter-level accuracy. Real-time measurements done without any corrections provided by a service like CPOS, typically have an accuracy of several meters.

This service is provided by the Norwegian Mapping Authority, but there are several other providers as well. The way it works is that the rover (user) sends the approximate position-data to the provider, and when the control-center receive the data, there is created a Virtual Reference Station (VRS). This station acts like a base-station nearby the rover, even though there are not any physical station there. The VRS is calculated by a computer using data from a network of base-stations, spread across Norway. To achieve optimal accuracy, it is recommended to be within 35 km of the closest reference-station. The base-stations are receiving signals from all available satellite constellations.

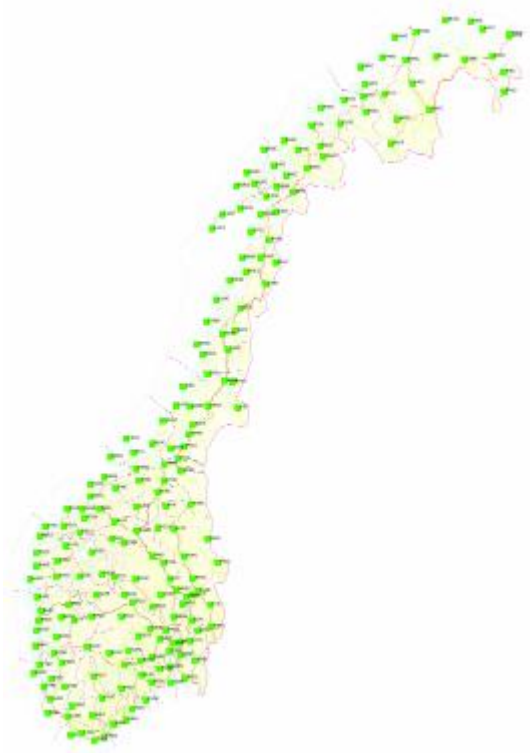

Figure 13 - All current base-stations (Kartverket, 2019)

CPOS is often used by surveyors where millimeter accuracy is unnecessary or does not make sense financially due to lack of benchmarks. Such applications include property-surveying, forestry, excavations, agriculture and more. (Kartverket, 2019)

2.6.2 ETPOS - Etter-Posisjonering

ETPOS is a service that is provided for free, for existing CPOS users. ETPOS is a server that contains raw observation-data from all the available base-stations. ETPOS means "**et**ter **pos**isjonering", when translated means post-positioning. Opposed to CPOS, ETPOS is offering to easily allow post-processing of data logged, without real-time corrections which is known as static measurements. This method requires the surveyor to do the measurements in the field, then later work on the post-processing. The advantage of doing this, is that you can achieve sub centimeter-level accuracy depending on the amount of time logged, compared to CPOS's centimeter-level.

2.6.3 IGS MGEX – International GNSS service Multi GNSS Experiment

IGS's webpage provides a variety of services, data, GNSS news and other resources. MGEX is one of their services, meaning **M**ulti-**G**NSS **Ex**periment, which track, collate and analyze all existing GNSS signals. Ranging from BeiDou, Galileo, GPS, GLONASS to even QZSS and NAVIC. And will provide precise ephemeris data and clock correction information from all the constellations mentioned above. Precise ephemeris is used for post-processing, to achieve even higher accuracy than you would using the broadcasted ephemeris that the satellites continuously transmit. The main difference between the two, is that the precise ephemeris needs to be calculated to be able to describe precisely how the satellites orbited the earth that given day, as well as if there are any differences in the clocks in the satellites and the ground control center's that day. The downside of using precise ephemeris is that it takes about 10-14 days to be calculated, and the gain in accuracy are in most cases miniscule. (Mgex.igs.org, 2019)

2.6.4 seSolstorm

seSolstorm is yet another service provided by *Kartverket*. This service use graphs in order to represent the amount of disruption in the ionosphere. If there is a high amount of disruption in the ionosphere, the accuracy of GNSS is reduced. Due to this being a possible threat to the accuracy of *Kartverket*'s other services, seSolstorm was created in order to give users a way to check if the quality is trustworthy. (Sesolstorm.kartverket.no, 2019)

2.6.5 GNSS Planning Online

GNSS planning online is a service provided by Trimble Inc, which is a reputable company within the GNSS-world. The site let users plan their GNSS projects, by using predicted satellite orbits and other variables in order to determine if the desired satellite coverage is present given location, that day. Along with satellite coverage, the tool can also provide dilution of precision (DOP) values, these values give an indication of whether the results are accurate or not. This planner can also provide ionospheric information. (Gnssplanningonline.com, 2019)

2.6.6 CenterPoint RTX Post-Processing

This service is also provided by Trimble Inc. CenterPoint RTX Post-Processing allows any user that register an account to post-process GNSS data for free, without needing a base station. This makes it one of many available Precise Point Positioning (PPP) services where users can upload observation files, and then get post-processing results delivered via e-mail. The way PPP services work is by using Rapid or Final satellite orbits and clock corrections in order to post-process the data. Then, automatically send a report back to the user. The reason why we chose to use this PPP service opposed to other services, is that Trimble was able to provide support for all RINEX formats, whereas other services only seemed to support RINEX 2. Trimble states that this service can provide an accuracy of less than 2cm horizontally. (Trimblertx.com, 2019) PPP calculations can also be done in software like *Leica Infinity* by downloading ephemeris manually from IGS, but we considered it more appropriate to use a PPP service in this thesis.

2.7 Hardware

2.7.1 Leica GS16

Leica Geosystems is one of the biggest suppliers of professional land-surveying equipment. GS16 is a multi-band and multi-constellation receiver. Hence why we chose the GS16 GNSS smart antenna for this project. The receiver contains several types of GNSS technologies like self-learning GNSS, which consists of adaptive on-the-fly satellite selection, as well as Leica's own NTRIP service, SmartLink. There is also continuous checking of RTK solution which according to the data sheet, have a 99.99% reliability. It also got signal tracking for all available GNSS constellations, plus 555 channels which allows more signals to be decoded at once, which gives fast acquisition and high sensitivity (Leica GS16 Data Sheet, 2016). The Leica Captivate software is user-friendly, giving a lot of possibilities in the field, ranging from easily customizable interface, to 2D and 3D models directly on the controller.

GS16 have a horizontal accuracy of 0.008m + 1 ppm and 0.015m + 1ppm vertically while using RTK, as well as horizontal accuracy of 0.003m + 0.1ppm and 0.0035m + 0.4ppm vertically, when using static measurements with long observations. (Leica GS16 Data Sheet, 2016)

Frequencies

The GS16 supports the following frequencies (Leica GS16 Data Sheet, 2016)

- GPS (L1, L2, L2C, L5)
- GLONASS (L1, L2, L2C, L3)
- BeiDou (B1, B2, B3)
- Galileo (E1, E5a E5b, alt-BOC, E6)
- QZSS (L1, L2, L5, L6)
- SBAS (WAAS, EGNOS, MSAS, GAGAN)

In other words, the GS16 can receive all available civilian signals, and this might be what gives Leica an advantage over u-blox. But if the price is worth the extra performance, is yet to be discussed.

2.7.2 U-blox ZED-F9P

Until recently, typical consumer GNSS-use was based on code or pseudo ranges; the C/A or coarse acquisition code of GPS on one frequency. GNSS-measurements based on carrier phase measurements on two frequencies was only available for special use, like land surveying. Until recently dual-frequency equipment was too expensive for the ordinary consumer. The last year, things have started to change. Some early signs were the introduction of dual-frequency support in the latest Android version, 8.0 / Oreo in summer 2017. Followed up by Broadcom introducing the BCM47755 dual frequency chipset. This does not mean that dual-frequency GPS quickly became the standard for mobile phones. (Price, 2019)

> So why is dual-frequency GNSS such a niche feature? The most likely answer is cost. Dual-frequency chips are not exactly commonplace at the moment, so it may be hard for manufacturers to get their hands on them. Another possible explanation is that vendors simply don't view it as an important feature.

As for now (March 2019) only the Huawei Mate 20-series and Xiaomi Mi8 run a dual-frequency GPS. Price is still a hinder. And the chips are locked to a mobile phone.

But things have changed in 2018. When we came up with the theme of our project it was unsure what type of GNSS-modules would be available for us. A bit of a change but with both Swift Navigation and u-blox introducing low-cost dual-frequency receivers. Swift navigation with a module and u-blox introducing the F9 platform. U-blox is a Swiss based company focusing on GNSS-positioning. The final step for us was Lithuania based CSG Shop offering a complete GNSS-module at the end of 2018 based on u-blox' F9 platform; the ZED-F9P.

The ZED-F9P is a multi-constellation and multi-band GNSS-module with the following specifications (ZED-F9P Data Sheet, 2019)

ZED-F9P Features:

Receiver type:

- 184-channel u-blox F9 engine
- GPS L1C/A L2C, GLO L1OF L2OF,
- GAL E1B/C E5b, BDS B1I B2I,
- QZSS L1C/A L2C

Nav. update rate:

- RTK up to 20 Hz1

Position accuracy:

- RTK 0.01 m + 1 ppm CEP

Convergence time:

- RTK < 10 sec
- Acquisition Cold starts 24 s
- Aided starts 2 s
- Reacquisition 2 s

Sensitivity:

- Tracking & Nav –167

- Cold starts –148 dBm
- Hot starts –157 dBm
- Reacquisition –160 dBm

With access to satellites from all four major actors and a promised position accuracy of 0.01 m + 1 ppm CEP, the module looked promising for our project. This in combination with the fact that u-blox provides its own software for configuring and testing u-blox platforms, and the fact that u-blox-based modules have a tiny but active community of users. Combining u-blox platforms with the RTKLIB-freeware made it perfect for our project.

Setup of the receiver based on the ZED-F9P

The ZED-F9P-devellopmentboard, is the core of our setup. In order to get a functional GNSS rover, we also need an antenna and controller. Since RTKLIB also has a version especially

developed for use on the Raspberry Pi with a touchscreen, choosing a Raspberry Pi as controller was the logical choice.

A capable antenna was a bit more difficult to get a hold of. There are a lot of GNSS-antenna types for sale but very often it is difficult to find out the details of the specifications. GNSS-antennas range from tiny magnetic for coarse purposes (car, motorbike etc.) to survey grade ones. Since it was important to have an antenna with a well-defined phase-center, we could focus on the latter ones. These types of antennas, often used for maritime purposes, gives the reason to believe that they are weather-resistant. We quickly discovered that the same antenna might have different specifications from different sellers. And since we wanted to include all four major satellite-systems on two frequencies, we needed to be sure that our antenna would support our requirements. We could not do much more than comparing specifications from different sellers and rely on the majority of reviews. Most sellers are service-minded, however it is difficult to test their technical knowledge about their products and their reliability.

Our final setup consists of an BT-152 antenna from BEITAN store on AliExpress, the previous described ZED-F9P and a RPi 3B+ with touchscreen as controller.

Figure 14 - Raspberry Pi 3 B+ (Photo by Desiré Trinborg, 2019)

Figure 14 shows the Raspberry Pi 3 B+ used in this project. The RPI is a single-board computer which have enough processing power for our use-case.

Figure 15 - Case for 5" Touch screen with Raspberry pi (Photo by Desiré Trinborg, 2019)

Figure 15 shows a picture of the controller we use for the ZED-F9P. As mentioned, the controller consists of the Raspberry Pi 3, and a 5" touchscreen. However, we needed some sort of protection for our hardware, therefore we 3D-printed a case.

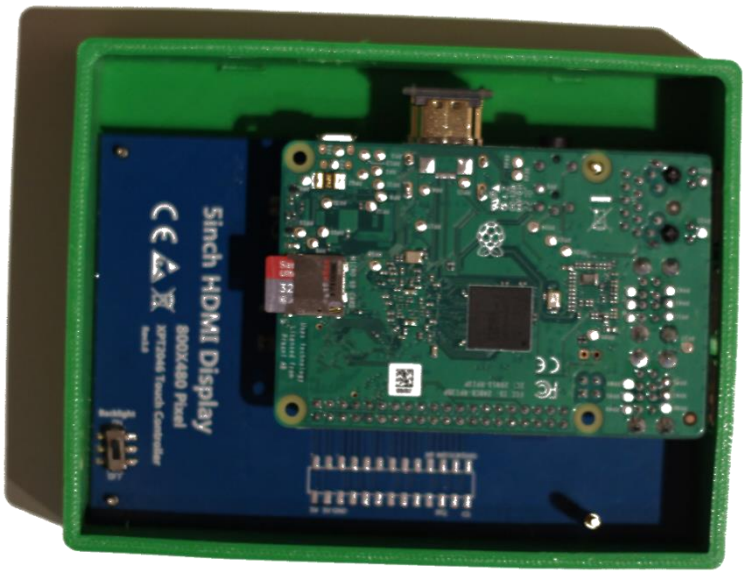

Figure 16 - Inside the case with hardware (Photo by Desiré Trinborg, 2019)

Figure 16 displays the 3D-printed case containing the Raspberry pi with the 5-inch touchscreen attached.

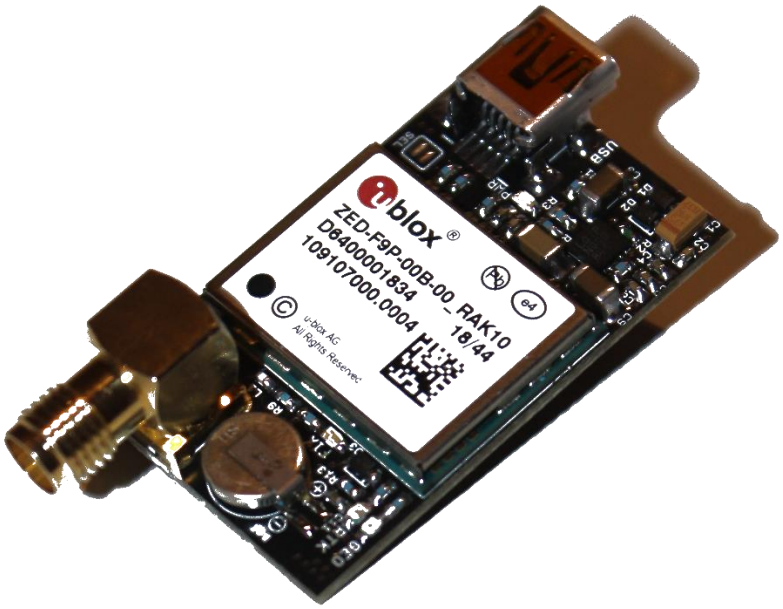

Figure 17 - ZED-F9P reciever module (Photo by Desiré Trinborg, 2019)

Figure 17 shows the centrepiece of the project, the ZED-F9P. There are different retailers that sell different boards with the F9P-chip attached. However, CSG shop was one of the first retailers to offer a fully operational board.

Figure 18 - TNC-SMA connector cable (Photo by Desiré Trinborg, 2019)

Figure 18 display the cables necessary to transfer data from the antenna to the u-blox-module.

Figure 19 – BT-152 (Photo by Desiré Trinborg, 2019)

Figure 19 shows the antenna we chose for the project. It was bought on AliExpress, and cost $45. Which is cheap considering the seller gives the following specifications for the antenna: (aliexpress.com, 2019)

> Supporting satellite signals: BeiDou: B1/B2/B3; GPS: L1/L2; GLONASS: G1/G2; Galileo: E1/E5b
>
> Working frequency range: 1197 MHz ~ 1278 MHz; 1559 MHz ~ 1605 MHz

Antenna Axis Ratio: < 3dB

Horizontal coverage angle: 360

Passive maximum gain: >3.5 dBic

Phase center error < 2.0 mm

Low noise amplifier gain: 40 + 2 dB

Noise figure: less than 1.5 dB

Output standing wave ratio: < 2.0 : 1

In-band flatness: +2 dB

The one thing lacking in the specifications is the phase center. The location of the phase center is quite important, which makes it strange that there is little information provided (our sellers were not able to dig up the necessary information either). Based on the typical construction of a GNSS-antenna board, it can be assumed that the phase center is in the vertical axis for the horizontal plane. As for the vertical plane it is less obvious, but it is possible to make a good assumption.

The antenna is made up of two halves, a top and a bottom part. It seems to be logical to place the antenna board in between the two parts. This is also seen with pro-GNSS antennas, where the phase center is located at the broader part of the antenna. Based on this we assume that the phase center is located 4.1 cm above the mount screw. It is possible to speculate about the lack of this information. The antenna is constructed for maritime use and in maritime situations there are not much need for information about the vertical location of the phase center. If our assumption is correct, then this will be confirmed with our measurements.

Figure 20 - Pinwheel Dual frquency GNSS-antenna (NovAtel inc, 2019)

Frequencies

system	Bands	
GPS	L1 X	1575.42±12MHZ (1563--1587)
	L2 X	1227±12MHZ (1215--1239)
	L5	1176±12MHZ (1164--1188)
	L6	1545±5MHZ (1540--1550)
GLONASS	G1 X	1609±7MHZ (1602--1616)
	G2 X	1252±7MHZ (1245--1259)
Beidou 1	L	1616MHZ (TX,LHCP)
	S	2491MHZ (RX,RHCP)
Beidou 2 (Compass)	B1 X	1561±2MHZ (1558--1563)
	B2 X	1207±10MHZ (1192--1219)
	B3 X	1268±10MHZ (1259--1278)
Galileo	L1	1575±17MHZ (1563--1587)
	L6	1545±5MHZ (1540--1550)
	E1 X	1609MHZ (1592--1609)
	E2	1561MHZ (1558--1561)
	E5 X	1192±15MHZ (1164--1215)
	E6	1278±12MHZ (1266--1290)

Figure 21 - Frequency table for the BT-152 (Shenzhen Beitian Communication Co. Ltd, 2019)

The marked frequencies should be available with the BT-152. But the frequency range from the specifications gives reason to believe that other Galileo-frequencies might be supported by the antenna as well.

```
G   12 C1C L1C D1C S1C C2L L2L D2L S2L C2M L2M D2M S2M      SYS / # / OBS TYPES
R    8 C1C L1C D1C S1C C2C L2C D2C S2C                     SYS / # / OBS TYPES
E    8 C1C L1C D1C S1C C7Q L7Q D7Q S7Q                     SYS / # / OBS TYPES
J    8 C1C L1C D1C S1C C2L L2L D2L S2L                     SYS / # / OBS TYPES
C    4 C2I L2I D2I S2I                                     SYS / # / OBS TYPES
```

Figure 22 - Observation list from a RINEX-file logged with u-blox

Figure 22 shows the different frequencies and observables received by the u-blox. The first column lists the different constellations G, R, E, J and C for GPS, GLONASS, Galileo, QZSS and BeiDou. The second one lists the number of different observables followed by the types of messages and a number for the frequency band. As an example, L1C stands for the new civilian code on 1575 MHz. The third last, L2M is the new military code on 1227 MHz.

For Galileo we can see the L7Q, which is a pilot signal, yet with no data, on the E5-band or 1192 MHz. The list confirms that our setup meets the necessary requirements for our project; being able to measure on dual frequencies against multiple constellations. Interesting enough, the header also shows that we received a signal from a Japanese QZSS-satellite even though their satellites have their workspace in Asia-Oceania.

```
G   12 C1C L1C D1C S1C C2W L2W D2W S2W C5Q L5Q D5Q S5Q      SYS / # / OBS TYPES
R    8 C1C L1C D1C S1C C2P L2P D2P S2P                      SYS / # / OBS TYPES
E   16 C1C L1C D1C S1C C5Q L5Q D5Q S5Q C7Q L7Q D7Q S7Q C8Q  SYS / # / OBS TYPES
       L8Q D8Q S8Q                                         SYS / # / OBS TYPES
C    8 C1I L1I D1I S1I C7I L7I D7I S7I                      SYS / # / OBS TYPES
```

Figure 23 – Observation list from a RINEX-file logged with a Leica GS16

Comparing *Figure 22* with the observation-list from *Figure 23*, shows that the Leica has more observables. Leica stand out with being able to receive triple-frequency for GPS and Galileo which might improve the Leica-rover's accuracy compared to the ZED-F9P.

3 Method

3.1 Planning

The focus of our measurements is on the pillars around the former football pitch behind the Smaragd-building of the NTNU in Gjøvik. They are meant to be the foundation. Previous there were four benchmarks made up of four pillars numbered 5261 to 6264. Benchmark 5262 didn't survive the building activity around the Smaragd-building and there is some uncertainty about the original position of 5261. As for now the three remaining pillars are numbered as Søyle 1 to Søyle 3 (*Figure 24*) or S1, S2 and S3.

The reason why we chose those benchmarks, is that we regard them as the most stable benchmarks in the close vicinity of the NTNU and that they meet some other requirements as different grades of free sight. The pillars are anchored 2.5 meters below ground level, which should be enough to keep them below the frost line. This is important due to water freezing in the ground has enough force to dislocate the pillars both in the horizontal and vertical plane.

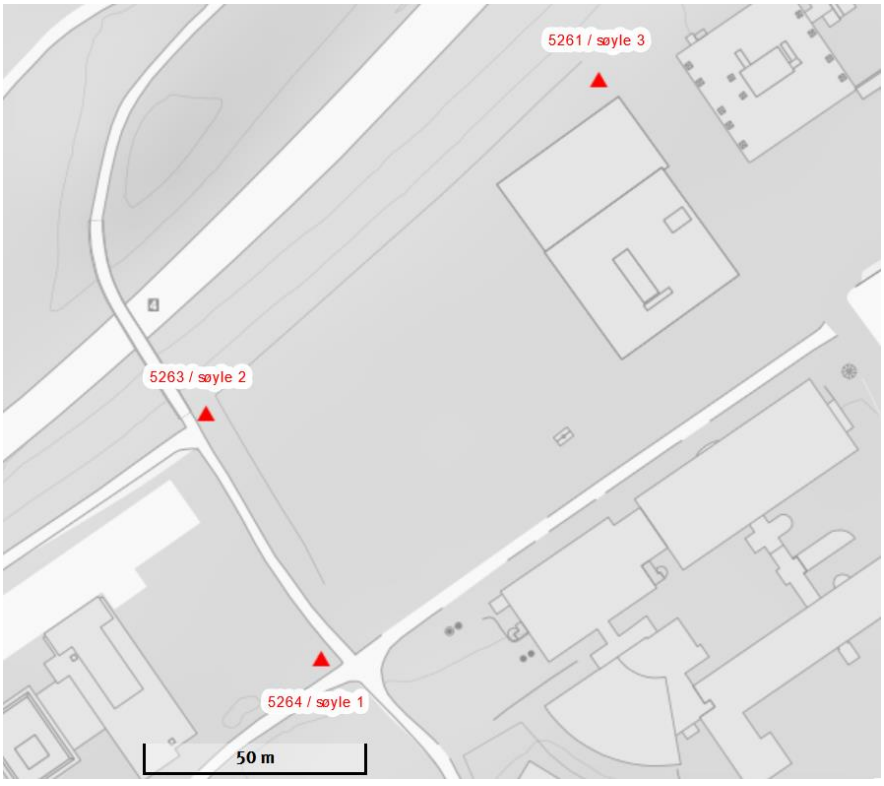

Figure 24 - Location of the benchmarks on Campus, S1 (søyle 1), S2 (søyle 2) and S3 (søyle 3).

Figure 25 - S1 (Photo by Marius Bredesen, 2019)

Figure 26 - S2 (Photo by Marius Bredesen, 2019)

Figure 27 - S3 (Photo by Marius Bredesen, 2019)

We assume the available coordinates for the benchmarks as unreliable. The benchmarks were re-established late autumn 2018, but due to uncertainty in the quality of the benchmarks from the Norwegian national network used in the analysis and adjustment calculations, we do not regard the results as adequate for our goal.

We decided to re-establish the benchmarks with 24-hour logging with GNSS. This method is chosen with the *Norwegian Mapping Authority*'s standard (Satelittbasert Posisjonsbestemmelse, 2009) in mind, 24-hour measurements provide the highest expected accuracy of; 2-4 mm with 2σ within 95%.

Logging for a longer period might improve the accuracy, but the gain will not stand against the increase of complexity due to the need of other external power sources. To be able to measure continuously for 24 hours, an option is to borrow external power supplies from Leica Norway. External power supplies are expected to last for at least 24 hours. To be able to do 24-hour measurements with our own setup, we decided to use a car battery with USB outlets.

24-hour static logging on all the three pillars with Leica-rovers, became the foundation for the analysis. We also logged for 24 hours with our own setup. The next step was static logging for shorter timespans, in order to predict the decrease of accuracy with shorter timespan

loggings; 6-hour, 3-hour and 1-hour logging. The previous mentioned standard from the Norwegian Mapping Authority provides oversight of what to expect from the methods.

In order to do the post processing, we will need observation data from at least three base stations. Our choice for building our networks around four stations, is a balance between what is necessary and what is workable. Adding a fourth station, increases the chance to check for errors in the measurements. However, adding more stations will lead to more prolonged processing. Keeping in mind that our aim is to check out the performance of the ZED-F9P, not to establish a watertight network, we consider four base stations as enough for our purposes.

Shorter base lines may provide better results. Our first choice became the following four base stations:

- DOKK, located near Dokka.
- MOEC, located near Moelv.
- SKRC, located near Skreia.
- KVM4, located near Hamar.

During the start of the analysis, problems occurred with the processing of the vector based on measurements with the u-blox towards KVM4. Infinity could not establish vectors based on phase fix, only on code messages or pseudo-range. The reason for this, might be due to KVM4 only logging GPS and GLONASS data. Therefore, we replaced KVM4 with LOTC which is located at about the same distance from Gjøvik as DOKK, ca. 35 km.

Our final list of base stations is:

- DOKK, located near Dokka.
- LOTC. Located near Løten.
- MOEC, located near Moelv.
- SKRC, located near Skreia.

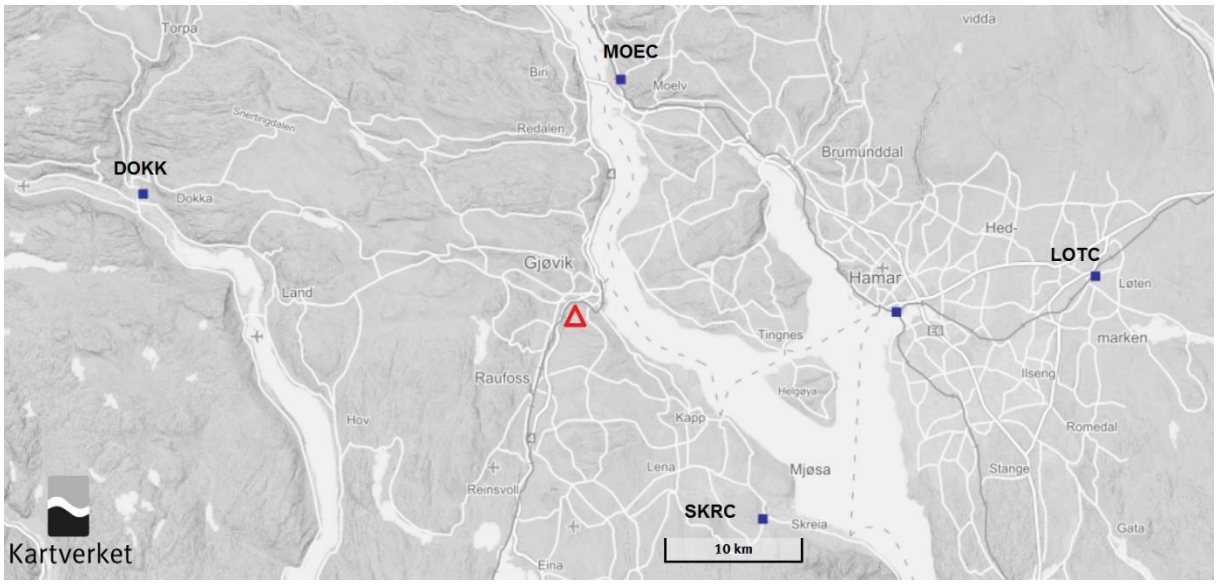

Figure 28 - map with overview of the base stations we used in our networks and the approximate location of our benchmarks marked with the red triangle

Changing from KVM4 to LOTC, lead to a minor problem. Data from ETPOS is only available for a period of three weeks in the RINEX 3 format we were using. By the time we figured out the cause of our problems with KVM4, the data for the first 7-8 hours of our 24-hour logging on the 11th and 12th of March, was not available anymore. This meant that we only could use RINEX 2 for LOTR for the 11th March. It is difficult to estimate the possible influence of lacking data for Galileo and BeiDou, but we consider it unlikely to be more than a few millimeters.

Table 1 – Overview of all the static measurements with al dates in 2019 + GPS day

Date	Benchmark	Instrument	Logging period
12th March / day 70&71	S1	Leica GS16	24 hours
19th March / day 77&78	S2	Leica GS16	24 hours
12th March / day 70&71	S3	Leica GS16	24 hours
19th March / day 77&78	S1	u-blox ZED-F9P	24 hours
12th March / day 70&71	S2	u-blox ZED-F9P	24 hours
19th March / day 77&78	S3	u-blox ZED-F9p	24 hours
15th March / day 74	S1	Leica GS16	6 hours
15th March / day 74	S2	Leica GS16	6 hours
21st March / day 80	S3	Leica GS16	6 hours
21st March / day 80	S1	u-blox ZED-F9P	6 hours
21st March / day 80	S2	u-blox ZED-F9P	6 hours
15th March / day 74	S3	u-blox ZED-F9P	6 hours
22nd March / day 81	S1	Leica GS16	3 hours
22nd March / day 81	S2	Leica GS16	3 hours
21st March / day 80	S3	Leica GS16	3 hours
21st March / day 80	S1	u-blox ZED-F9P	3 hours

21st March /day 80	S2	u-blox ZED-F9P	3 hours
22nd March / day 81	S3	u-blox ZED-F9P	3 hours
22nd March / day 81	S1	u-blox ZED-F9P	1 hour
22nd March / day 81	S2	u-blox ZED-F9P	1 hour
22nd March / day 81	S3	u-blox ZED-F9P	1 hour
22nd March / day 81	S1	Leica GS16	1 hour
22nd March / day 81	S2	Leica GS16	1 hour
22nd March / day 81	S3	Leica GS16	1 hour

3.1.1 GNSS planning online and seSolstorm:

Until recently, one could mainly use the satellites from GPS and GLONASS. Nowadays, both Galileo and BeiDou can be considered fully operational, which means that we have the opportunity to use satellites from four constellations. The ETPOS-service includes BeiDou and Galileo. It is usual to plan and check the available satellites and other parameters, which might influence the measurements on forehand with a GNSS-planner. We used Trimble's online-version. Due to the increased availability of satellites from BeiDou and Galileo, the need for extensive planning might have become less important when it comes to the available number of satellites. However, until this become a new accepted and established standard, GNSS-planning is still a part of the procedure.

System: active		Satellites	
		Selected	Healthy
GPS	✔	31	31
GLONASS	✔	24	24
Galileo	✔	22	22
BeiDou	✔	39	39
QZSS	✖	0	3
IRNSS	✖	0	7

Figure 29 - Selected satellite systems (Gnssplanningonline.com, 2019)

My Settings Change settings

Time of almanac:	2019-03-11
Time zone:	UTC +01:00
Visible period:	
2019-03-11 16:00 - 2019-03-12 16:00	
Latitude:	N 60° 47' 20.1897"
Longitude:	E 10° 40' 46.2304"
Height:	2 m
Elevation cutoff:	15 °

Figure 30 - General settings (Gnssplanningonline.com, 2019)

Since our goal was logging for 24 hours, we decided to extend the logging with 30 minutes as an insurance to have measured for the full 24 hours. The GNSS-planner does not exceed a 24-hour period; therefore, information will be lacking for a small period. The graphs will show that this does not impact the result. In order to confirm this, we checked the graphs for the following day.

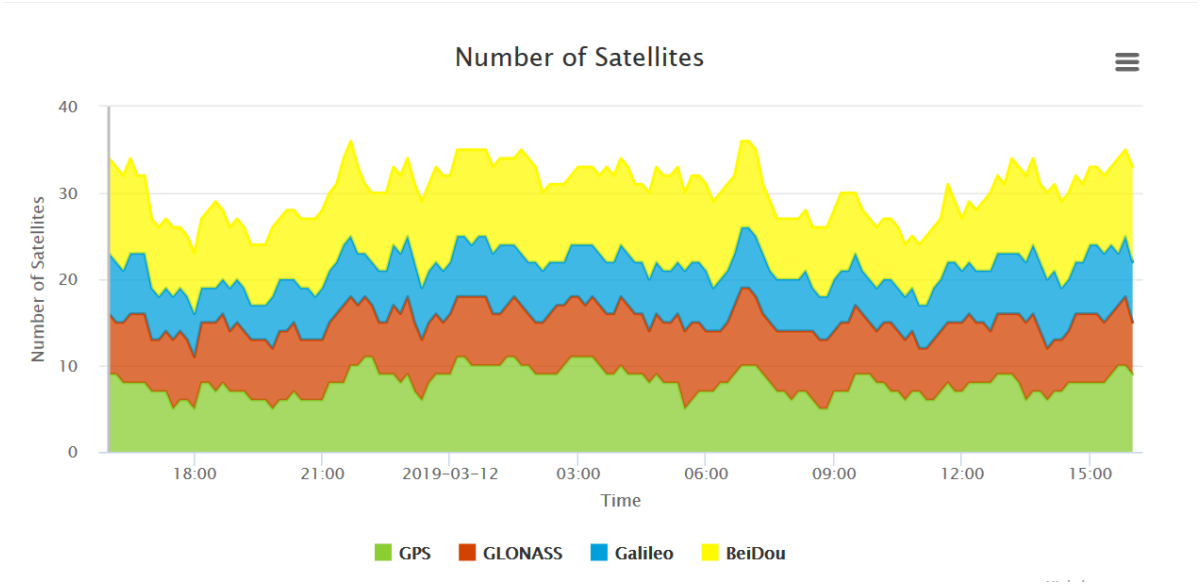

Figure 31 - Available satellites in planned period (Gnssplanningonline.com, 2019)

Figure 31 shows that there were at least 23 satellites available during the measurements.

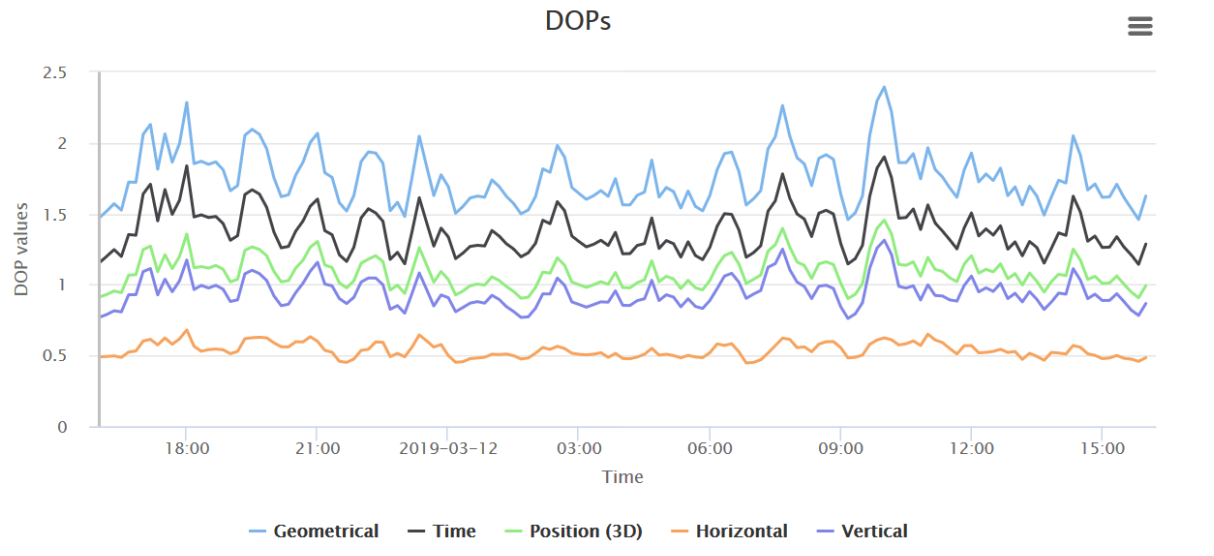

Figure 32 - Dilution of precision values (Gnssplanningonline.com, 2019)

Figure 32 shows that the theoretical DOP-values were below 2.5 for the whole period.

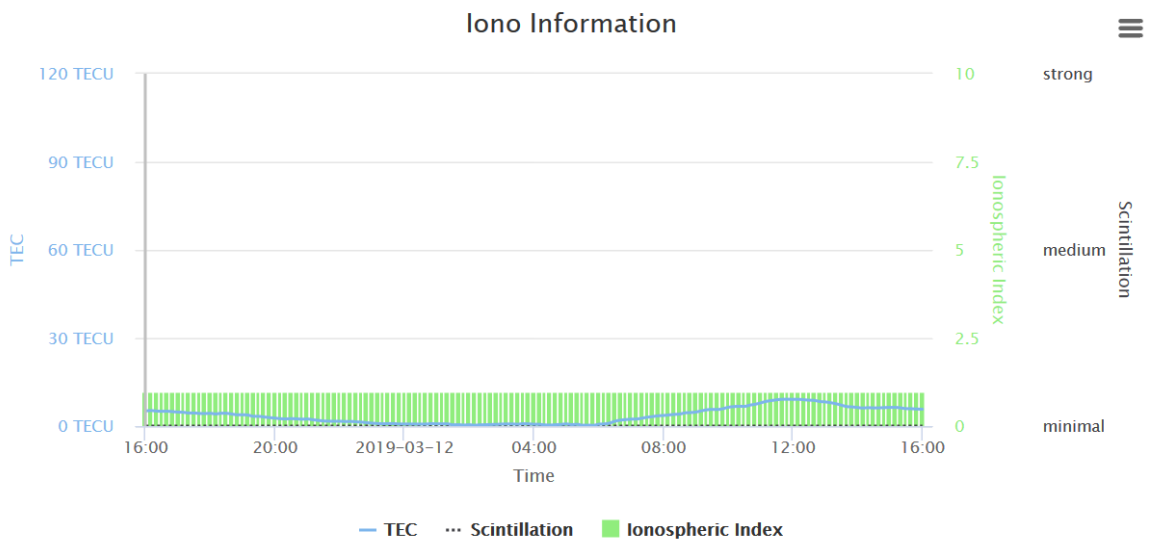

Figure 33 - Ionospheric information (Gnssplanningonline.com, 2019)

Figure 33 shows low ionospheric activity. This can be confirmed at *seSolstorm*. Maps of ionospheric disturbances are based on measurements and it is difficult to predict for an extended period of time. *seSolstorm* provides the actual situation and has an archive to check conditions for a given date and time. With navigation buttons, it is possible to navigate through the archive with 5 minutes or 1-hour leaps.

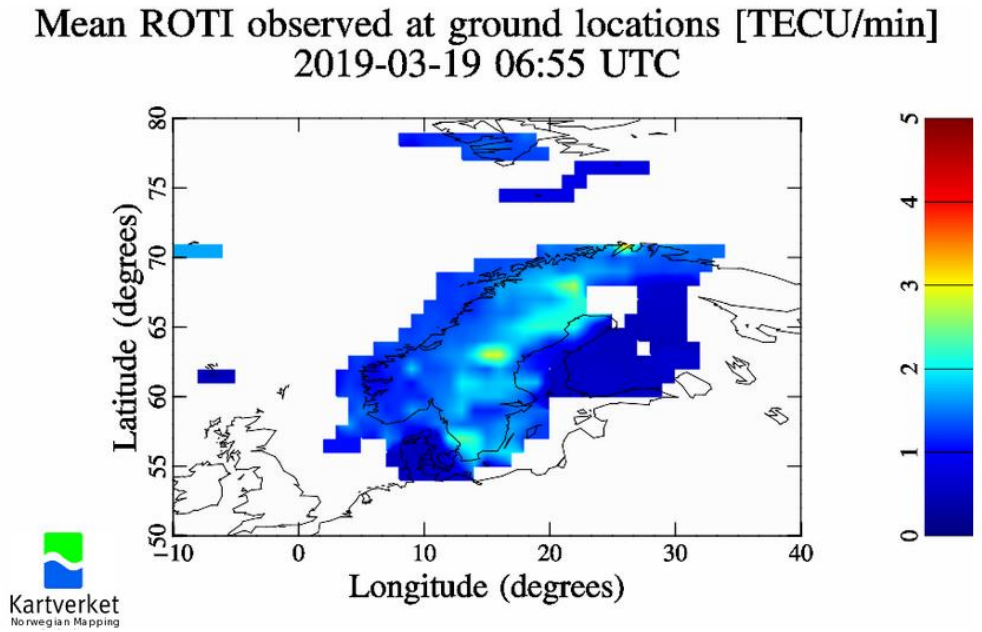

Figure 34 - Plot showing mean ROTI observed on the 19th of March 06:55 (Sesolstorm.kartverket.no, 2019)

Figure 34 shows a plot with moderate disturbances. Kartverket writes the following (Sesolstorm.kartverket.no, 2019, own translation):

> Disturbances on the ground
>
> This figure shows the amount of ionospheric disturbance observed by receivers on the ground. Turbulent ionosphere causes serious disturbances in GNSS signals. These disturbances may not be removed and may cause issues for all types of GNSS systems. The legend ranges from blue towards red, where blue is low to none turbulence, and red is high turbulence.

Highly turbulent ionosphere will cause disturbance in the satellite signals. These kinds of disturbances can usually not be corrected with post processing. Checking hourly plots is time consuming and *seSolstorm* provides 24-hour graphs showing the mean TEC (Total Electron Content) Index rate at ground level:

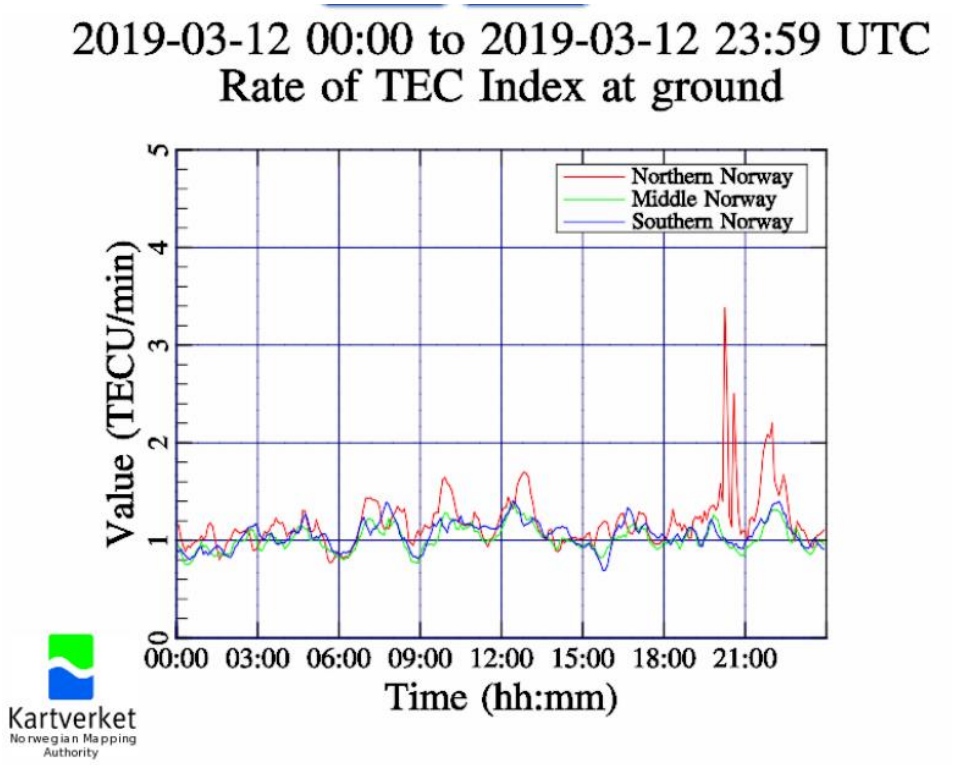

Figure 35 - Mean TEC Index rate at ground level for 12th of March (Sesolstorm.kartverket.no, 2019)

The blue line shows low activity for our measurements on the 19th of March. The 24-hour graphs do not show any significant level of ROTI (Ionospheric turbulence) during our measurements. The red line in *Figure 35* shows high activity in northern Norway at the end of the period. By checking the map plots, it is possible to figure if this might have interfered with the measurements

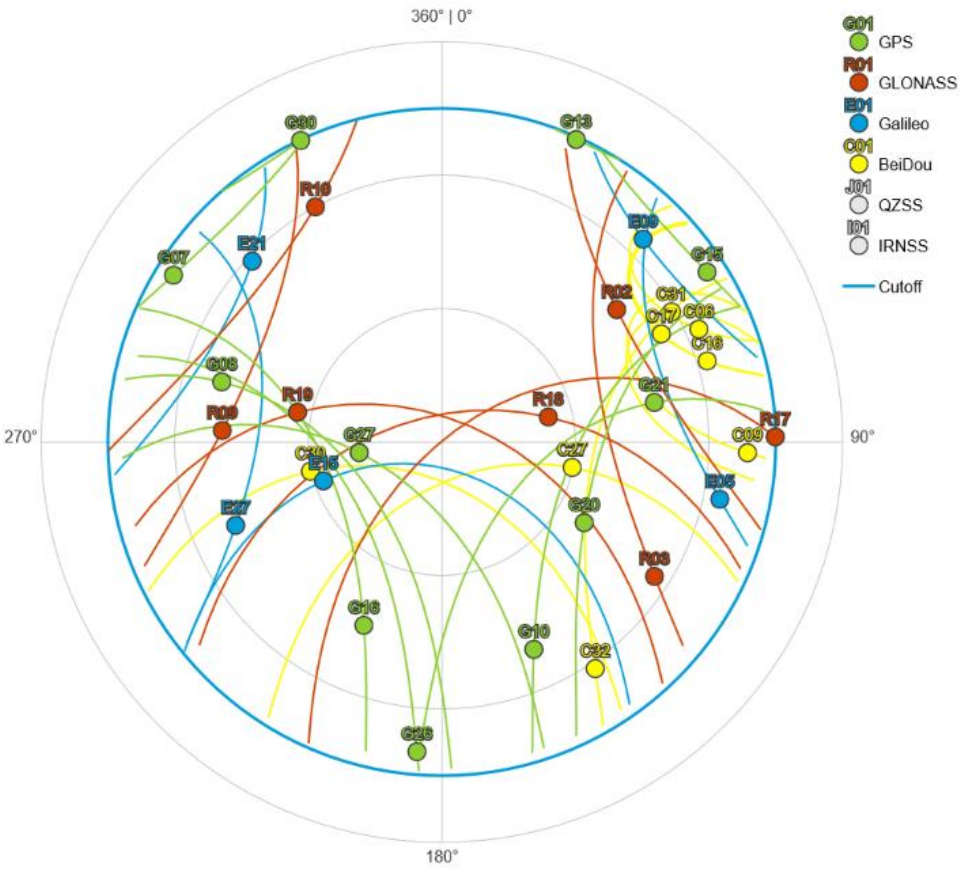

Figure 36 – Skyplot (Gnssplanningonline.com, 2019)

The sky plot shows an even spreading of satellites at a given time. This supports the theoretical DOP-values.

Set up Leica

There are some different tutorials on how to set up the Leica GS16 for raw data logging. We found Greg Perkins tutorial (Perkins, 2017) to be a useful.

It was chosen to use all the available signals from all four satellite systems. This should give plenty of available satellites. We chose a cut off angle of 15°. The cut off angle is the angle below where satellites no longer are taken into the solution. The signals from satellites with a low elevation, have a longer travel through the earth's atmosphere and are likely to be disturbed by this. Usually there are objects like buildings, trees or hills in the surroundings which might disturb the signals. The cut off angle becomes a balance between tracking as

many satellites as possible, without tracking satellites that might give unreliable measurements. A cut off angle of 15° is widely used, but with a surplus of satellites it should not be necessary to choose lower cut off angles. Parameters which might cause breaks during logging like DOP-limits, quality check and automatic stop of point measurements are checked 'off'. We wanted to log static for 24-hours, and logged data directly into the rover's SD-card, with an interval of one second and only point observations. Logging data to the internal memory, hides all settings for the controller due to our decision to start recording observations as soon as the sensor was switched on. The controller is not used at all after the set up.

Besides GNSS-planning in advance, we also checked the weather conditions in advance. Our measurements were done during Norwegian winter. Even though GNSS-antennas do not tend to be disturbed by a tiny layer of snow, a thicker layer on the antenna-surface may cause errors especially on coordinate-heights. The antennas in the base stations from the *Norwegian Mapping Authority* are dome shaped, under dry snow conditions it is not likely that snow can settle on the antennas. The antennas we used are dish shaped and may collect a layer of snow. During our first 24-hour measurement, we experienced light snow for shorter periods, which had to be brushed away to prevent snow settling on the antennas.

RTK-STATIC

RTKLIB provides the possibility to connect to a NTRIP-server, therefore we wanted to test the performance of the ZED-F9P with RTK-measurements. *The Norwegian Mapping Authority* provided us with a login for their CPOS-network. Due to issues with the setup and connecting with CPOS, changes had to be made in the RTKLIB-software. The community and Franklin, one of the creators of RTKBASE (RPI based RTKLIB) have been helpful to customize code with information we provided. Due to Franklin's code updates, we might have been some of the first to test the new functionalities of RTKLIB. As a result, we were not aware of what to expect.

The RTK-CPOS measurements were kept simple. We decided to do classic static RTK measurements on the three pillars, in order to compare the resulting coordinates with the coordinates from our previous 24-hour loggings. The measurements consist of 10 conclusive fixes with 2 second intervals, repeated 3 times randomly.

RTK-DYNAMIC

To test the possibilities for using the ZED-F9P for dynamic purposes, we decided to do a test by measuring over a shorter distance. We chose a route starting with clear view in all directions, continuing into a forested area with irregular geography. The length was approximately one kilometre; measured with low speed (ca. 5 km/h) and an interval of 5 seconds. The set up was kept simple with a weighted pole in order to keep the antenna as horizontal as possible. The focus was to be positioned in a horizontal plane. Variations in height was neglected. We tried as good as possible to keep the same distance from the side of the road to test the lane level accuracy of the module.

PPP

Considering the ZED-F9P is a relatively cheap GNSS-module, we wanted to explore the cheapest alternative towards achieving centimeter accuracy. Which as of now would be through free precise point positioning services. This makes an F9P owner able to collect data and upload it to a website to achieve centimeter accuracy, without having to pay for software or any sort of subscription service to achieve good results. We ended up using Trimble's service, *CenterPoint RTX Post-Processing* for this part, due to Trimble supporting the RINEX 3 format.

4 Results

4.1 Static measurements

In the following chapters the results of the measurements are presented with point-ID S1, S2 and S3, the receiver Leica or u-blox, the length of the measurement and the adjusted coordinates. The adjusted coordinates are the coordinates calculated in the adjustment analysis as described in chapter 5. The coordinates are in the EUREF89 UTM – zone 32. EUREF89 UTM is one of the two standard coordinate systems for geomatics in Norway. EUREF89 UTM consists of 60 zones which cover the whole globe. The zones 32 to 35 cover the Norwegian mainland and Svalbard (Spitsbergen).

For every set of measurements for a given timespan (24, 6, 3 and 1 hour) there is also presented a table which shows the deviation for the coordinates of the actual measurements compared with the 24-hour measurements with Leica.

4.1.1 24 Hours

Leica

Table 2 - Results using Leica setup (EUREF89 UTM32 NN2000)

Point ID	Receiver	Duration	North	East	Height
S1	Leica	24 Hours	6740381,0174	591414,0258	185,4701
S2	Leica	24 Hours	6740432,8968	591387,5064	183,4651
S3	Leica	24 Hours	6740518,2794	591466,5444	184,1467

U-blox

Table 3 - Results using u-blox setup (EUREF89 UTM32 NN2000)

Point ID	Receiver	Duration	North	East	Height
S1	u-blox	24 Hours	6740381,0200	591414,0204	185,4719
S2	u-blox	24 Hours	6740432,8943	591387,5092	183,4841
S3	u-blox	24 Hours	6740518,2718	591466,5445	184,1473

Difference between 24 hours measurements

Table 4 - Difference in coordinates between Leica and u-blox 24h (Meters)

Point ID	Receiver	Δ North	Δ East	Δ Height
S1	u-blox	0,0026	-0,0054	0,0018
S2	u-blox	-0,0025	0,0028	0,0190
S3	u-blox	-0,0076	0,0001	0,0006

4.1.2 6 Hours

Leica

Table 5 - Results Leica 6 hours (EUREF89 UTM32 NN2000)

Point ID	Receiver	Duration	North	East	Height
S1	Leica	6 Hours	6740381,0161	591414,0225	185,4654
S2	Leica	6 Hours	6740432,8969	591387,5146	183,4682
S3	Leica	6 Hours	6740518,2740	591466,5428	184,1407

U-blox

Table 6 - Results u-blox 6 hours (EUREF89 UTM32 NN2000)

Point ID	Receiver	Duration	North	East	Height
S1	u-blox	6 Hours	6740381,0230	591414,0265	185,4755
S2	u-blox	6 Hours	6740432,8886	591387,5134	183,4700
S3	u-blox	6 Hours	6740518,2704	591466,5435	184,1405

Difference between 24 hours Leica measurements

Table 7 - Differences in coordinates between Leica 6h and Leica 24h (Meters)

Point ID	Receiver	Δ North	Δ East	Δ Height
S1	Leica	0,0007	0,0033	-0,0047
S2	Leica	-0,0001	-0,0082	0,0031
S3	Leica	0,0054	0,0016	-0,0060

Table 8 - Difference in coordinates between u-blox 6h and Leica 24h

Point ID	Receiver	Δ North	Δ East	Δ Height
S1	u-blox	0,0056	-0,0007	0,0054
S2	u-blox	-0,0082	0,0070	0,0049
S3	u-blox	0,0090	0,0009	-0,0062

4.1.3 3 Hours

Leica

Table 9 - Results of Leica 3h (EUREF89 UTM32 NN2000)

Point ID	Receiver	Duration	North	East	Height
S1	Leica	3 Hours	6740381,0158	591414,0241	185,4609
S2	Leica	3 Hours	6740432,8979	591387,5154	183,4662
S3	Leica	3 Hours	6740518,2709	591466,5409	184,1323

U-blox

Table 10 - Results of u-blox 3h (EUREF89 UTM32 NN2000)

Point ID	Receiver	Duration	North	East	Height
S1	u-blox	3 Hours	6740381,0240	591414,0230	185,4670
S2	u-blox	3 Hours	6740432,8963	591387,5115	183,4705
S3	u-blox	3 Hours	6740518,2762	591466,5474	184,1495

Difference between 24 hours Leica measurements

Table 11 Differences in coordinates between Leica 3h and Leica 24h

Point ID	Receiver	Δ North	Δ East	Δ Height
S1	Leica	0,0016	0,0017	-0,0092
S2	Leica	-0,0011	-0,0090	0,0011
S3	Leica	0,0085	0,0035	-0,0144

Table 12 - Differences in coordinates between u-blox 3h and Leica 24h

Point ID	Receiver	Δ North	Δ East	Δ Height
S1	u-blox	0,0066	-0,0028	-0,0031
S2	u-blox	0,0005	-0,0051	0,0054
S3	u-blox	0,0032	-0,0030	0,0028

4.1.4 1 Hour

Leica

Table 13 - Results of Leica 1h (EUREF89 UTM32 NN2000)

Point ID	Receiver	Duration	North	East	Height
S1	Leica	1 Hour	6740381,0166	591414,0260	185,4633
S2	Leica	1 Hour	6740432,8956	591387,5141	183,4706
S3	Leica	1 Hour	6740518,2747	591466,5392	184,1549

U-blox

Table 14 - Results og u-blox 1h (EUREF89 UTM32 NN2000)

Point ID	Receiver	Duration	North	East	Height
S1	u-blox	1 Hour	6740381,0122	591414,0268	185,4694
S2	u-blox	1 Hour	6740432,8889	591387,5106	183,4713
S3	u-blox	1 Hour	6740518,2700	591466,5504	184,1393

Difference between 24 hours Leica measurements

Table 15 - Differences in coordinates between Leica 1h and Leica 24h

Point ID	Receiver	Δ North	Δ East	Δ Height
S1	Leica	0,0008	-0,0002	-0,0068
S2	Leica	-0,0012	-0,0077	0,0055
S3	Leica	0,0047	0,0052	0,0082

Table 16 - Differences in coordinated between u-blox 1h and Leica 24h

Point ID	Receiver	Δ North	Δ East	Δ Height
S1	u-blox	0,0052	-0,0010	-0,0007
S2	u-blox	0,0079	-0,0042	0,0062
S3	u-blox	0,0094	-0,0060	-0,0074

4.2 Real time kinematic results

U-blox real time kinematic results

Table 17 - Results real-time kinematic measurements (EUREF89 UTM 32 NN2000)

Point ID	Receiver	Method	North	East	Height
S1	u-blox	Real-time	6740381,0150	591414,0260	185,4760
S1	u-blox	Real-time	6740381.0140	591414.0220	185.4550
S1	u-blox	Real-time	6740381.0130	591414.0240	185.4730
S2	u-blox	Real-time	6740432,9010	591387,5160	183,4520
S2	u-blox	Real-time	6740432.9870	591387.4380	187.7930
S2	u-blox	Real-time	6740432.9970	591387.4490	182.8080
S3	u-blox	Real-time	6740518,2670	591466,5460	184,1480
S3	u-blox	Real-time	6740518.2610	591466.5480	184.1520
S3	u-blox	Real-time	6740518.2580	591466.5570	184.1510

Leica static 24 hours for reference

Table 18 - Results 24h static measurements for reference (EUREF89 UTM32 NN2000)

Point ID	Receiver	Method	North	East	Height
S1	Leica	24 Hours	6740381,0174	591414,0258	185,4701
S2	Leica	24 Hours	6740432,8968	591387,5064	183,4651
S3	Leica	24 Hours	6740518,2794	591466,5444	184,1467

Differences between U-blox RTK and Leica static 24 hours

Table 19 - Comparison between 24h static and real-time measurements (Meters)

Point ID	Δ North	Δ East	Δ Height
S1	0,0054	-0,0002	0,0059
S1	0,0034	0,0038	-0,0151
S1	0,0044	0,0018	0,0029
S2	-0,0042	-0,0096	-0,0131
S2	-0,0902	0,0684	4,3279
S2	-0,1002	0,0574	-0,6571
S3	0,0124	-0,0016	0,0013
S3	0,0184	-0,0036	0,0053
S3	0,0214	-0,0126	0,0043

4.2.1 Real time kinematic – Dynamic results

Figure 37 shows the results of the dynamic RTK-measurements with an orthophoto as background-layer. Some points were too far away from the route and can therefore not be seen in the figure. Those points will be discussed later under *RTK-Dynamic*.

Figure 37 - Orthophoto with dynamic RTK-measurements

4.3 Precise Point Positioning results

4.3.1 Geocentric coordinates

Table 20 - Results from PPP service, coordinates is geocentric given in reference frame ETRS89 (Trimblertx.com, 2019)

Point ID	Receiver	Method	X	Y	Z
S1	u-blox	PPP	3066794,415	578320,002	5544066,070
S2	u-blox	PPP	3066753,045	578286,600	5544089,991
S3	u-blox	PPP	3066666,816	578352,958	5544131,227

4.3.2 Geographic coordinates

Table 21 - Results from PPP service based on 1-hour measurements with ZED-F9P, coordinates are geographic for easier comparison with static measurements. Reference frame is ETRS89 (Trimblertx.com, 2019)

Point ID	Receiver	Method	Latitude (N)	Longitude (E)	Height
S1	u-blox	PPP	60° 47' 18.01427	10° 40' 44.87224	224.306
S2	u-blox	PPP	60° 47' 19.71232	10° 40' 43.20950	222.324
S3	u-blox	PPP	60° 47' 22.40519	10° 40' 48.57559	222.964

Table 22 - Geographic coordinates from Leica 24h measurements for reference (WGS84 reference frame)

Point ID	Receiver	Method	Latitude (N)	Longitude (E)	Height
S1	Leica	PPP	60° 47' 18.01	10° 40' 44.87	224.2420
S2	Leica	PPP	60° 47' 19.71	10° 40' 43.21	222.1899
S3	Leica	PPP	60° 47' 22.40	10° 40' 48.58	222.9113

5 Analysis

5.1 Introduction

Our measurements between the 12th and the 22nd of March gave us 24 datasets ranging from 1- to 24-hour static raw data.

As described under Planning, we expect the 24-hour measurements to be the foundation for the analysis. We can then assume the resulting coordinates as close to the absolute value, and further compare the results of other measurements.

> This method is chosen with background in *Statens Kartverk'*s standard "Satellittbasert posisjonsbestemmelse" noting -presis enkeltpunktbestemmelse med logging av rådata på to frekvenser over en periode på 24 timer med etterprosessering- as the method with highest expected accuracy; 2-4 mm with 2σ within 95%.

The main analysis is done in Leica Infinity. Leica Infinity is a rather new software which can handle a wide range of data formats from a wide range of different types of instruments. As Leica infinity is a relatively new software, our experience was not sufficient and became somewhat of a problem. After being in contact with both Leica Norway and Leica Geosystems in Switzerland, we believe we have come to a working method in order to produce, analyze and compare the data and results from our measurements. The parameters we used are based on the information we retrieved from various manuals and support pages.

5.2 Adjustment Calculations

We chose the following parameters for the adjustment calculations. In *Leica Infinity*.

General:

Controls:	Constrained (advised by manual)
Confidence levels:	Height 1D – 68.3% (default)
	Error ellipses 2D – 95.0% (advised by manual for GNSS adjustment)
Iterations:	Max. 3 (default)
	Iteration criteria 0.0001 m (default)

TPS accuracy information:

Default values

Level accuracy information:

Default values

Test criteria:

Level of significance:	5% (default)
Power of test (1-β):	80% (default)
-σ a-posteriori-:	Use/Ignore

Advanced terrestrial parameters:

Default values

GNSS accuracy information:

Source for standard deviations:	Individual (advised by manual)
Centering height errors:	Default values
-σ a priori (GNSS)-:	Adjusted for passing the F-test and Chi-test and

We focused on three test results in the summary. Since the *σ a priori* was set to 1.0 (which is usual), we aimed to achieve -*σ a-posteriori* at roughly the same value. At the same time, we wanted the F-test and the Chi-test to pass within the tolerance values. To achieve this, we could adjust the -*σ a priori* (GNSS)-value to a level which hopefully would make the three tests pass. In general, the longer the observations, the higher we had to scale -*σ a priori* (GNSS)- in order to pass the tests. This is expected, due to the multitude of observations that gives unrealistically low standard deviations.

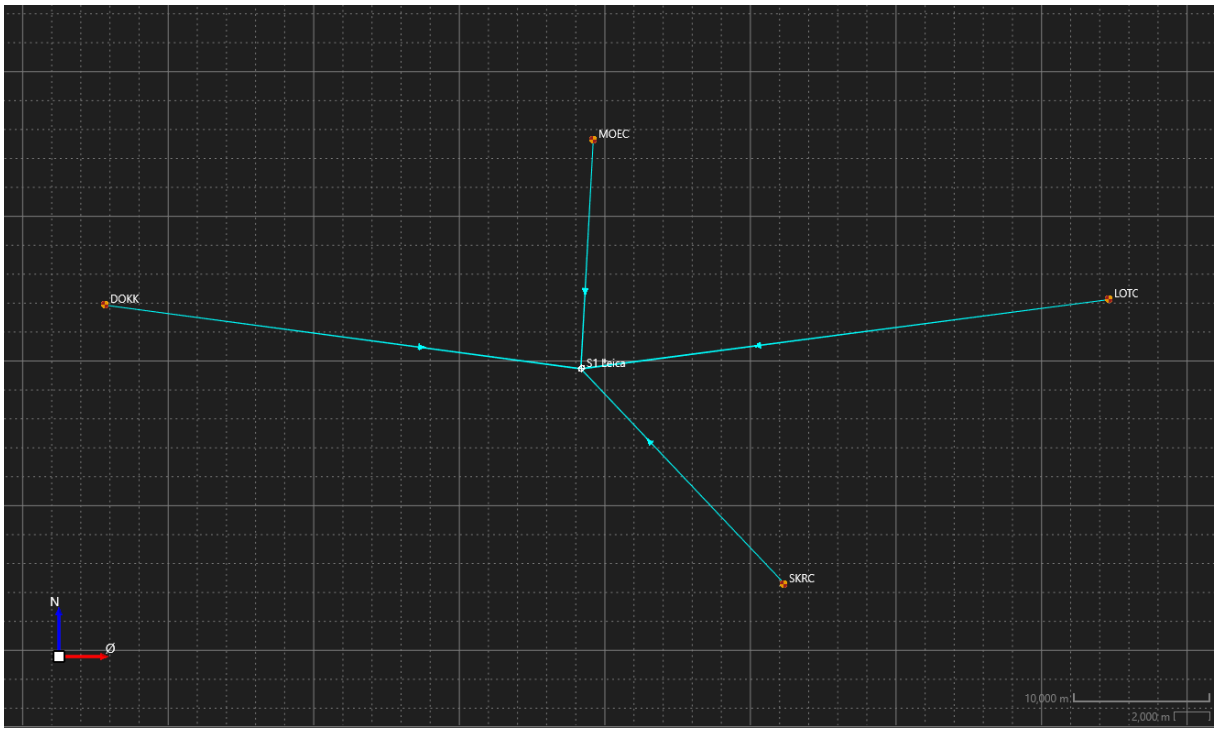

Figure 38 - Overview of our networks with the base stations DOKK, LOTR, MOEC and SKRC

As *Figure 38* shows, our networks are based on four base stations from *Statens Kartverk*, which are located to the north, east, west and south of our benchmarks with vectors from the base stations to the benchmarks. The base stations from *Statens Kartverk* have been logging

their position constantly, for a long period of time. We consider the Norwegian Mapping Authority's coordinates to be highly reliable. Noting that due to the ongoing process of land rise after the last ice age, the heights of the base stations may change over time. This is taken into consideration by *the Norwegian Mapping Authority* and will not influence our measurements. The four base stations make up our control points in the analysis, and we have assumed that their coordinates are absolute when using them as control points. Therefore, we decided to not remove any control points. We started the analysis by adjusting freely without constraints in order to test the observations. In the free adjustment, some observations were flagged, due to too high values to pass the tests. The normal procedure would be to remove the observation and re-run the adjustment in order to check for improvements. But as in real life surveying analysis, removing one observation may result in the errors propagating to other observations. Our networks were small, with few points. We made the decision to not remove any observations at all in continuing the analysis process. Since our networks were small, removing any of the points would weaken the network. The second reason was that some observations did not pass the test values but was not far above the tolerance values. The third reason was that we could not see a clear pattern in the rejecting of the observations by the tests; they seem to be spread over the vectors to all four base stations.

σ a-posteriori:	**0.946**
Tester	
Tol.verdi W-test:	1.96
Tol.verdi T-test (2-dimensjonal):	2.42
Tol.verdi T-test (3-dimensjonal):	1.89
Tol.verdi F-test:	1.04
F-test:	0.90
Chi kvadratstest (95.0%)	
Nedre toleransegrense:	0.46
Øvre toleransegrense:	1.75
Chi kvadratstest:	0.90

Figure 39 - critical values for W, T and Chi-test

As we can see in *Figure 39,* the critical values for T and W-test are respectively 1.89 and 1.96. In *Figure 40,* we can see that the observation from LOTC-S2 and SKRC are flagged red, due to the test-values being above the tolerance values. When we look at the estimated values for the errors and compare them with the MDB for the observations, all the estimated errors are below the values for the MDB. The MDB, or minimal detectable bias, reflects the internal

reliability. The MDB is the smallest possible size an error in an observation can have, and still be detectable by the statistical tests. High values for the MDB give poor reliability of the observations. Therefore, it will be difficult to check for outliers or gross errors.

Observasjonstester

	Stasjon	Målepunkt	MDB	Rød	BNR	W-test	Est. feil	T-test
ΔX	MOEC	S1 Leica 24t 1203	0.0036 m	29	4.45	-0.01	-	0.02
ΔY			0.0026 m	30	4.33	0.12	-	-
ΔZ			0.0067 m	26	4.75	0.16	-	-
ΔX	DOKK	S1 Leica 24t 1203	0.0033 m	20	5.69	-1.16	-	0.46
ΔY			0.0024 m	21	5.54	-0.06	-	-
ΔZ			0.0062 m	18	6.06	0.63	-	-
ΔX	SKRC	S1 Leica 24t 1203	0.0035 m	26	4.83	-0.03	-	0.35
ΔY			0.0025 m	26	4.73	1.02	-	-
ΔZ			0.0065 m	23	5.17	-0.14	-	-
ΔX	LOTC	S1 Leica 24t 1203	0.0038 m	25	4.92	1.39	-	0.95
ΔY			0.0026 m	25	4.87	-1.10	-	-
ΔZ			0.0071 m	22	5.29	-0.74	-	-
ΔX	MOEC	S3 Leica 24t 1203	0.0040 m	57	2.41	0.58	-	0.32
ΔY			0.0029 m	57	2.42	-0.85	-	-
ΔZ			0.0077 m	60	2.28	-0.24	-	-
ΔX	SKRC	S3 Leica 24t 1203	0.0039 m	56	2.45	0.13	-	0.16
ΔY			0.0028 m	57	2.43	0.40	-	-
ΔZ			0.0075 m	60	2.31	-0.56	-	-
ΔX	LOTC	S3 Leica 24t 1203	0.0042 m	62	2.16	-0.87	-	1.39
ΔY			0.0029 m	58	2.36	0.65	-	-
ΔZ			0.0080 m	63	2.12	1.91	-	-
ΔX	DOKK	S3 Leica 24t 1203	0.0037 m	54	2.55	0.11	-	0.38
ΔY			0.0027 m	55	2.52	-0.19	-	-
ΔZ			0.0071 m	58	2.38	-0.95	-	-
ΔX	LOTC	S2 UBX 24t 1203	0.0060 m	72	1.70	-0.97	-0.0021 m	2.03
ΔY			0.0043 m	73	1.71	0.85	0.0013 m	-
ΔZ			0.0113 m	75	1.60	-1.51	-0.0061 m	-
ΔX	DOKK	S2 UBX 24t 1203	0.0054 m	68	1.95	1.75	-	1.80
ΔY			0.0039 m	67	1.95	0.38	-	-
ΔZ			0.0095 m	65	2.06	0.29	-	-
ΔX	SKRC	S2 UBX 24t 1203	0.0055 m	67	1.99	-0.12	-	1.81
ΔY			0.0040 m	67	1.97	-2.16	-0.0031 m	-
ΔZ			0.0099 m	66	2.00	0.94	-	-
ΔX	MOEC	S2 UBX 24t 1203	0.0054 m	63	2.12	-0.75	-	0.46
ΔY			0.0039 m	63	2.14	0.96	-	-
ΔZ			0.0098 m	64	2.10	0.07	-	-

Figure 40 - Observation tests from the adjustment report for 24-hours on the 12th March (Attachment)

Leica's manual (Advanced Network Adjustment, 2017) writes the following:

> 5. There might be cases that an observation is marked as a possible outlier, but the estimated error is small –even smaller than the MDB value for this observation. In such cases, it is up to the user to decide whether this observation is really an outlier or not.

The adjustment report from the 6-hour logging on the 21st March, show a similar pattern. In *Figure 41*, we see that the observations MOEC-S1 and MOEC-S3 are flagged with values slightly too high for the T-test (the tolerance values remain the same as for the 24-hour

measurements). However, there are no reason to remove the observations from the data, as the estimated errors are below the MDB-values for the observations (as shown in *Figure 41*).

Observasjonstester

	Stasjon	Målepunkt	MDB	Rød	BNR	W-test	Est. feil	T-test
ΔX	SKRC	S3 Leica 6t 2103	0.0037 m	29	4.38	1.56	-	0.89
ΔY			0.0027 m	26	4.72	-0.55	-	-
ΔZ			0.0067 m	33	3.94	-0.37	-	-
ΔX	DOKK	S3 Leica 6t 2103	0.0036 m	30	4.20	-1.15	-	0.78
ΔY			0.0027 m	29	4.43	-0.77	-	-
ΔZ			0.0065 m	34	3.83	0.81	-	-
ΔX	MOEC	S3 Leica 6t 2103	0.0036 m	29	4.35	-1.64	-0.0021 m	**1.95**
ΔY			0.0027 m	27	4.66	1.87	0.0018 m	-
ΔZ			0.0066 m	34	3.91	-0.01	0.0000 m	-
ΔX	LOTC	S3 Leica 6t 2103	0.0035 m	27	4.57	1.20	-	0.52
ΔY			0.0026 m	24	5.06	-0.54	-	-
ΔZ			0.0064 m	30	4.26	-0.44	-	-
ΔX	DOKK	S1 UBX 6t 2103	0.0039 m	52	2.70	0.29	-	1.40
ΔY			0.0029 m	53	2.62	1.69	-	-
ΔZ			0.0070 m	50	2.79	-1.08	-	-
ΔX	LOTC	S1 UBX 6t 2103	0.0037 m	51	2.75	-0.98	-	0.40
ΔY			0.0028 m	55	2.53	0.49	-	-
ΔZ			0.0069 m	53	2.66	0.77	-	-
ΔX	MOEC	S1 UBX 6t 2103	0.0039 m	54	2.61	1.89	0.0026 m	**1.90**
ΔY			0.0029 m	54	2.55	-1.75	-0.0018 m	-
ΔZ			0.0070 m	51	2.76	-0.45	-0.0011 m	-
ΔX	SKRC	S1 UBX 6t 2103	0.0040 m	56	2.48	-1.18	-	0.65
ΔY			0.0030 m	57	2.40	-0.46	-	-
ΔZ			0.0072 m	54	2.59	0.79	-	-
ΔX	DOKK	S2 UBX 6t 2103	0.0060 m	69	1.95	1.45	-	1.70
ΔY			0.0044 m	65	2.07	-1.33	-	-
ΔZ			0.0094 m	63	2.14	0.29	-	-
ΔX	MOEC	S2 UBX 6t 2103	0.0059 m	68	1.97	-0.21	-	0.20
ΔY			0.0047 m	70	1.83	-0.43	-	-
ΔZ			0.0097 m	67	2.00	0.63	-	-
ΔX	SKRC	S2 UBX 6t 2103	0.0060 m	68	1.95	-0.75	-	1.46
ΔY			0.0047 m	70	1.84	1.67	-	-
ΔZ			0.0097 m	66	2.02	-0.52	-	-
ΔX	LOTC	S2 UBX 6t 2103	0.0058 m	67	2.00	-0.48	-	0.27
ΔY			0.0046 m	69	1.89	0.16	-	-
ΔZ			0.0094 m	65	2.07	-0.40	-	-

Figure 41 - Observation test from adjustment report 6h 21th of March (Attachement)

Observasjonstester

	Stasjon	Målepunkt	MDB	Rød	BNR	W-test	Est. feil	T-test
ΔX	MOEC	S1 Leica 24t 1203	0.0117 m	80	1.41	1.75	-	1.25
ΔY			0.0086 m	80	1.38	-0.62	-	-
ΔZ			0.0207 m	80	1.40	-0.22	-	-
ΔX	DOKK	S1 Leica 24t 1203	0.0098 m	65	2.05	**-3.78**	-0.0133 m	**5.82**
ΔY			0.0073 m	66	2.00	**2.22**	0.0057 m	-
ΔZ			0.0175 m	66	2.04	1.95	0.0122 m	-
ΔX	SKRC	S1 Leica 24t 1203	0.0109 m	76	1.58	0.68	-	0.29
ΔY			0.0081 m	77	1.55	-0.60	-	-
ΔZ			0.0194 m	76	1.58	-0.57	-	-
ΔX	LOTC	S1 Leica 24t 1203	0.0115 m	79	1.44	**1.98**	0.0082 m	1.87
ΔY			0.0081 m	77	1.53	-1.30	-	-
ΔZ			0.0203 m	78	1.45	-1.46	-	-
ΔX	MOEC	S3 Leica 24t 1203	0.0191 m	76	1.58	1.14	-	0.51
ΔY			0.0137 m	77	1.54	-0.39	-	-
ΔZ			0.0375 m	76	1.58	-0.14	-	-
ΔX	SKRC	S3 Leica 24t 1203	0.0186 m	74	1.66	0.27	-	0.08
ΔY			0.0135 m	75	1.60	-0.31	-	-
ΔZ			0.0367 m	75	1.65	-0.38	-	-
ΔX	LOTC	S3 Leica 24t 1203	0.0205 m	80	1.39	0.73	-	0.25
ΔY			0.0138 m	77	1.54	-0.54	-	-
ΔZ			0.0393 m	79	1.45	-0.41	-	-
ΔX	DOKK	S3 Leica 24t 1203	0.0178 m	70	1.84	-1.95	-	1.59
ΔY			0.0128 m	71	1.78	1.16	-	-
ΔZ			0.0352 m	71	1.80	0.87	-	-
ΔX	LOTC	S2 UBX 24t 1203	0.0314 m	80	1.37	0.35	-	0.20
ΔY			0.0225 m	80	1.40	-0.21	-	-
ΔZ			0.0591 m	83	1.29	-0.73	-	-
ΔX	DOKK	S2 UBX 24t 1203	0.0281 m	74	1.68	-0.98	-	0.54
ΔY			0.0205 m	74	1.67	0.85	-	-
ΔZ			0.0497 m	71	1.77	0.70	-	-
ΔX	SKRC	S2 UBX 24t 1203	0.0283 m	74	1.66	0.10	-	0.13
ΔY			0.0207 m	74	1.64	-0.61	-	-
ΔZ			0.0510 m	74	1.67	-0.04	-	-
ΔX	MOEC	S2 UBX 24t 1203	0.0276 m	72	1.76	0.56	-	0.12
ΔY			0.0200 m	72	1.76	-0.05	-	-
ΔZ			0.0502 m	72	1.73	-0.05	-	-

Figure 42 - extract from constraint adjustment 24-hour 12th March, scaled to 120 (Attachment)

Figure 42 contain the same dataset as *Figure 40*. But *Figure 42* is from a constraint adjustment calculation. This means that we have set the base stations as control points and locked the coordinates. Now, *Leica Infinity* can only adjust the points S1, S2 and S3. We can now see that there are other observations flagged. The tolerance values remain the same, and now the observations DOKK-S1 and MOEC-S1 are flagged for the W-test, and DOKK-S1 is flagged for the T-test. As for the W-test, the results are just slightly above, but the T-test for DOKK-S1 is higher than the tolerance value of 1.89. We can also see that the estimated error is -0.0133 m and when we compare this with the MDB for the same observation (0.0098), it makes the observation a possible outlier.

Previously, we stated that we would need severe reasons in order to remove any observations, as it would weaken the network. We tried removing the DOKK-S1 observation, in order to try to tell if this is a gross error, but as seen earlier in the analysis, the errors are just propagating

to other observations. This leads us to stick with the decision to not remove observations continuing the analysis process.

There are two more values in the report that might be useful. The Leica's manual (Advanced Network Adjustment, 2017) writes the following:

> 1. It is desirable that the BNR is homogeneous for the entire network
>
> 3. Always strive to retain sensibly small MDB values or else the network might become very insensitive in detecting outliers.
>
> 4. It is advised that the Red value exceeds 20 for all observations.

As the MDB reflects the internal reliability, the BNR or bias to noise ratio reflects the external reliability. It expresses the maximum influence of an undetected error on the adjusted coordinates. It is clear that the BNR is closely related to the MDB. High values for the MDB give poor reliability, and the risk of a gross error or outliers not being detected increases. A homogenous distribution of the BNR-points in a network, gives possibilities to check for errors.

The Red value, or redundancy value, express the rate of controllability of observations. High values equal good controllability of observations.

As mentioned, there seems to be a clear relation between the length of the logging and the need for scaling of the -σ *a priori* (GNSS). This applies to measurements with the Leica GS16 and the ZED-F9P, when it comes to both free and constraint adjustment. We also see that the measurements from logging with the u-blox in general do not require as high scaling as measurements with the Leica GS16, although there were some exceptions. We contacted Leica Support in Switzerland, who confirmed our procedure as technically correct, but they also questioned the high scaling, without reasoning or knowing why. The main reason for the scaling, was to achieve more reliable values for standard deviations. Scaling does not affect the statistical test or the quality of the points. Similar adjustment calculations were made for the remaining measurements.

As seen in *Table 1*, the measurements consist of measuring with one type of antenna (either Leica or u-blox) on two pillars at the same date and time, and logging with the same antenna type on the third pillar on a different day. In order to treat all the measurements as evenly as

possible, we made our final adjustment calculations for only one point at a time, along with our four control points.

From the first part of the analysis, it does not seem to be any gross errors in the observations. Along with our decision to not remove observations without a severe reason, we have made the final calculations to obtain the coordinate quality as constraint. To make sure we did not miss any outliers, all adjustments are checked for the results of the tests, and estimated errors are compared with the MDB-values.

5.3 Point quality results

Below, the coordinate quality of the measurements are presented grouped after the length of the measurements and the receiver. The tables show the calculated coordinate quality for the point ID in 3D, 2D and heights (1D). The coordinate quality (CQ) gives an indication of how high the accuracy of the points is, given in meters. In this thesis, coordinate quality given is the calculated value that 95% of all measurements is located within (also known as 2σ).

5.3.1 24-hour measurements

Leica

Table 23 - Point quality for Leica 24h (2σ)

Point-ID	3D-CQ [m]	2D-CQ [m]	1D-CQ [m]
S1	0.0061	0.0030	0.0053
S2	0.0065	0.0032	0.0056
S3	0.0059	0.0029	0.0051

U-blox

Table 24 - Point quality for u-blox 24h (2σ)

Point-ID	3D-CQ [m]	2D-CQ [m]	1D-CQ [m]
S1	0.0064	0.0032	0.0056
S2	0.0054	0.0027	0.0047
S3	0.0053	0.0027	0.0046

5.3.2 6-hour measurements

Leica

Table 25 - Point quality for Leica 6h (2σ)

Point-ID	3D-CQ [m]	2D-CQ [m]	1D-CQ [m]
S1	0.0072	0.0037	0.0061
S2	0.0072	0.0036	0.0062
S3	0.0088	0.0046	0.0075

U-blox

Table 26 - Point quality for u-blox 6h (2σ)

Point-ID	3D-CQ [m]	2D-CQ [m]	1D-CQ [m]
S1	0.0091	0.0048	0.0077
S2	0.0083	0.0044	0.0071
S3	0.0082	0.0041	0.0071

5.3.3 3-hour measurements

Leica

Table 27 - Point quality for Leica 3h (2σ)

Point-ID	3D-CQ [m]	2D-CQ [m]	1D-CQ [m]
S1	0.0074	0.0038	0.0064
S2	0.0072	0.0037	0.0062
S3	0.0061	0.0032	0.0052

U-blox

Table 28 - Point quality for u-blox 3h (2σ)

Point-ID	3D-CQ [m]	2D-CQ [m]	1D-CQ [m]
S1	0.0075	0.0038	0.0064
S2	0.0072	0.0036	0.0062
S3	0.0070	0.0037	0.0059

5.3.4 1-hour measurements

Leica

Table 29 - Point quality for Leica 1h (2σ)

Point-ID	3D-CQ [m]	2D-CQ [m]	1D-CQ [m]
S1	0.0099	0.0050	0.0085
S2	0.0087	0.0044	0.0076
S3	0.0091	0.0045	0.0079

U-blox

Table 30 - Point quality for u-blox 1h (2σ)

Point-ID	3D-CQ [m]	2D-CQ [m]	1D-CQ [m]
S1	0.0076	0.0038	0.0067
S2	0.0096	0.0052	0.0080
S3	0.0086	0.0048	0.0071

5.3.5 Visualization of point quality

All adjusted measurements for S1:

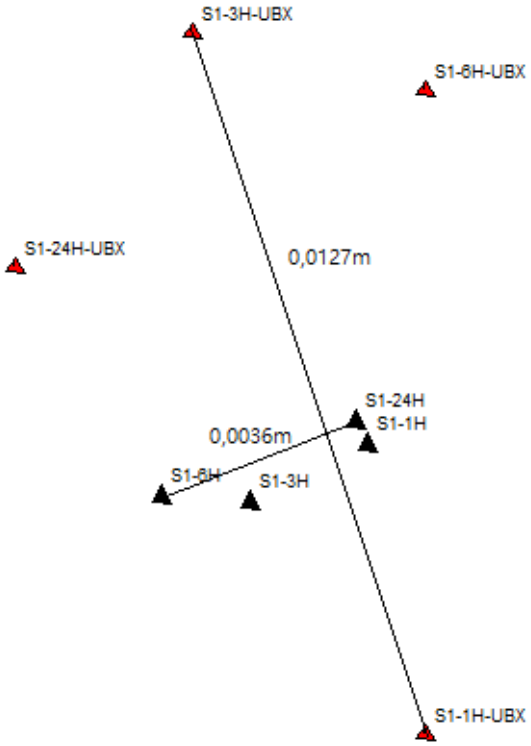

Figure 43 - Leica and u-blox measurements for S1 (Black = Leica, Red = u-blox)

As *Figure 43* - Leica and u-blox measurements for S1 (Black = Leica, Red = u-blox) shows, the measurements with the biggest difference for u-blox is 1-hour and 3-hour measurements, with the difference of 1,27cm. The figure also shows that the measurements with the biggest difference for Leica, is the difference between the 24h hour measurements and the 6-hour measurements.

All adjusted measurements for S2:

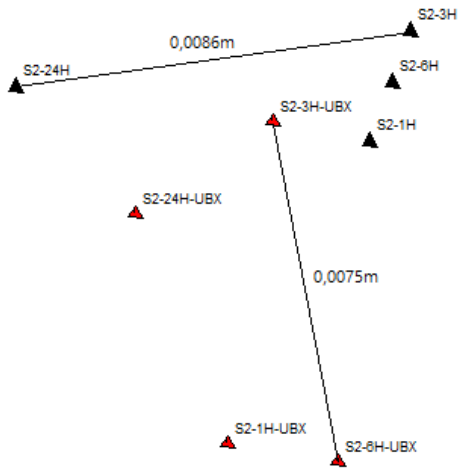

Figure 44 - Leica and u-blox measurements S2 (Black = Leica, Red = u-blox)

In *Figure 44*, the biggest differences for u-blox is between the 3-hour and 6-hour measurements. As for Leica, is it between the 24-hour measurements and the 3-hour. It is also worth mentioning that there are millimeter differences between all the points, but the GS16 is more consistent and precise with the sub-centimeter accuracy.

All adjusted measurements for S3:

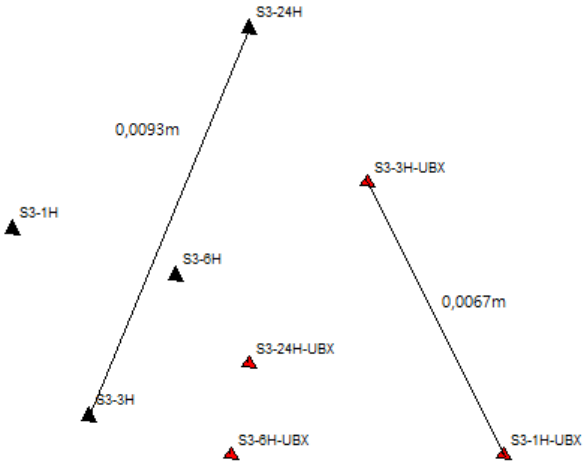

Figure 45 - Leica and u-blox measurements S3 (Black = Leica, Red = u-blox)

Figure 45 show biggest differences between the 3-hour and 1-hour measurements for u-blox, and once again between 24-hour and 3-hour for Leica.

5.4 RTK

5.4.1 Static pillar S1, S2 and S3

In *results*, we experienced mixed results when comparing the differences between real-time measurements and the 24-hours static measurements.

Table 31 - Differences between RTK and Static (EUREF89 UTM 32 NN2000)

Point ID	Δ North	Δ East	Δ Height
S1	0,0054	-0,0002	0,0068
S1	0,0034	0,0038	0,0151
S1	0,0044	0,0018	-0,0029
S2	-0,0042	-0,0096	0,0131
S2	-0,0902	0,0684	-4,3279
S2	-0,1002	0,0574	0,6571
S3	0,0124	-0,0016	-0,0013
S3	0,0184	-0,0036	-0,0053
S3	0,0214	-0,0126	-0,0043

In *Table 31* the differences are given in meters, and we experienced a 4,3279 meters gap in height at S2 in one of our three datasets. And 0,6571 meters in height for another measurement, both marked with red in *Table 31*. In other words, two of three datasets for S2 did not give desired accuracy for height, nor North and East.

The accuracy we can expect for real-time kinematic measurements is given by the Norwegian Mapping Authority which provides the corrections that allow real-time positioning to be:

Table 32 – Expected accuracy for 66% (1 sigma) of all measurements. (Kartverket, 2019)

Dimension	Areas with approx. 35km between SATREF PGS	Areas with approx. 70 km between SATREF PGS
2D (EUREF 89)	8 mm	14 mm
1D Ellipsoidal height	17 mm	30 mm
1D Height (NN2000)	20 mm	36 mm

In *Table 31* we see that the errors are ranging from 50mm to approximately 100mm in 2D for S2, which is higher than the 8 mm given in *Table 32*. Even if we were to multiply the values in *Table 32* by 2 in order to get accuracy values that would apply in 95% (2 sigma) of all measurements, the errors would still be too significant. The one remaining dataset for S2 passed the 95% threshold, and so did all the other datasets for S1 and S3.

The coordinates in *Table 17*, are the result of adjustment calculations in *GisLine Landmåling*. The instrument parameters necessary to calculate reasonable standard deviations, are chosen according to the specifications for the ZED-F9P given by the u-blox. Standard deviations for 2D and heights were set to 1 cm, according to the position accuracy. And centering accuracy for 2D and heights were set to 2 mm, according to the phase center error of < 2mm. For the centering accuracy for heights, it is worth noting that we had to manually calculate the location of the phase center, therefore this parameter might be slightly low in the software.

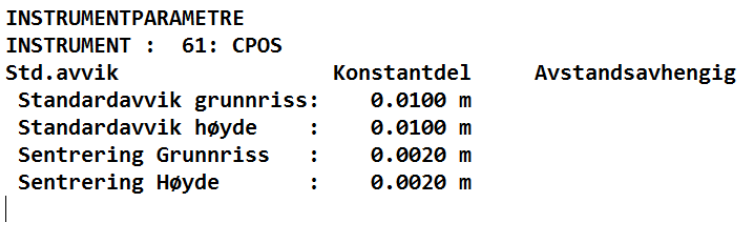

Figure 46 - Instrumentparametres in GISline

Considering that we probably were the first to test some new code for RTKLIB with corrections from a NTRIP-server. Our main concern was the precision of RTK. *Figure 47* shows the point-observation file used for the adjustment calculations, and there are sub-centimeter differences between the observations. The figure also shows that there are in total 10 conclusive measurements for point S1 with cartesian X, Y and Z coordinates.

```
-00 Formater for satellitt-vektorer på KOF-format
-45 SSSSSSSSS KKKKKKKK XXXXXXX.XXXX YYYYYYY.YYYY ZZZZZZZ.ZZZZ II.III Bk MMMMMMM
-00
 00 ------------ Satellite-vectors from : SKI, Leica -----------------
 00 @%Unit:               m
 00 @%Coordinate type:    Cartesian
 00 @%Reference ellipsoid: WGS 1984

 45 S1                 3066794.4130  578319.9940 5544065.9933  0.000
 45 S1                 3066794.4143  578319.9962 5544066.0021  0.000
 45 S1                 3066794.4130  578319.9943 5544065.9978  0.000
 45 S1                 3066794.4138  578319.9946 5544066.0013  0.000
 45 S1                 3066794.4130  578319.9920 5544065.9952  0.000
 45 S1                 3066794.4144  578319.9939 5544065.9990  0.000
 45 S1                 3066794.4156  578319.9942 5544065.9993  0.000
 45 S1                 3066794.4137  578319.9959 5544065.9991  0.000
 45 S1                 3066794.4110  578319.9925 5544065.9948  0.000
 45 S1                 3066794.4152  578319.9945 5544065.9954  0.000
```

Figure 47 - Observation-file showing cartesian coordinates for RTK on pillar 1

As mentioned, there is less than 1 cm difference in the measurements. This is graphically confirmed by importing the observations into GISline and measuring the distance between the outermost points.

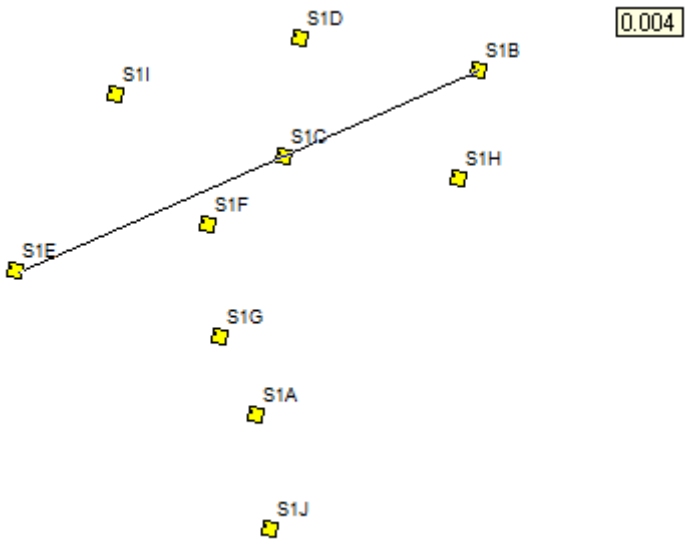

Figure 48 - There are 4mm difference between the outermost points in S1

5.4.2 Dynamic

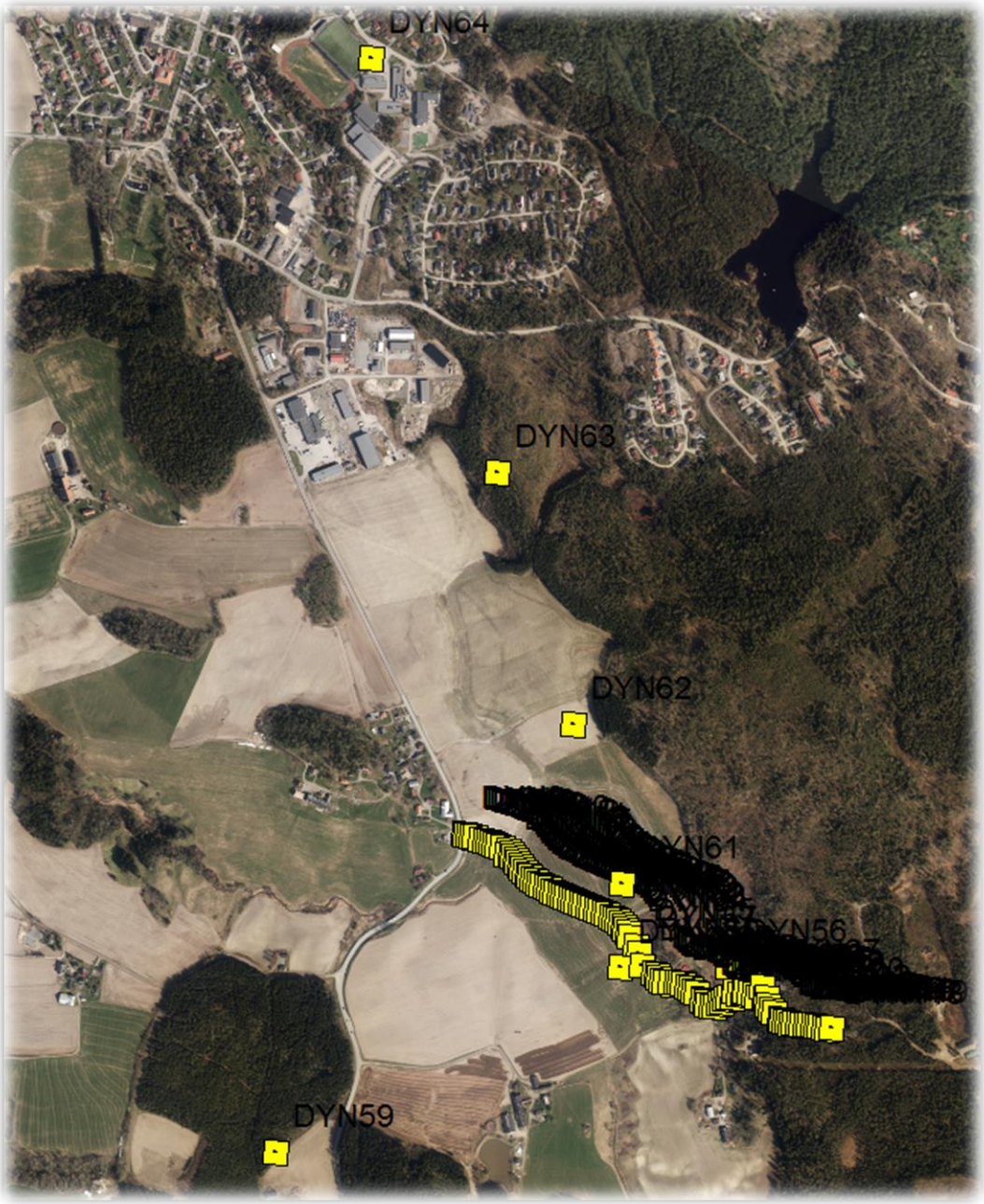

Figure 49 - All the point observations from the dynamic RTK-measurements.

Figure 49 shows all observations from the dynamic measurements, including four measurements which were far off from the route. The road lacks a clearly marked centerline, which would make it easier to analyze. Along with the fact that it is difficult to keep track of the right position on the road without a guiding system, the analysis will be based on estimations of positions and distances.

Taking a closer look at the first half of the route, we can see that the points in general keep a rather constant distance from the roadside, apart from DYN41 which is slightly disorientated.

Figure 50 - Detail of the first half of the route; points DYN17-DYN54

Looking even closer at points DYN42 to DYN53, we can see the ZED-F9P to keep track of its position (at least relatively). The next part of the route caused some issues for our setup:

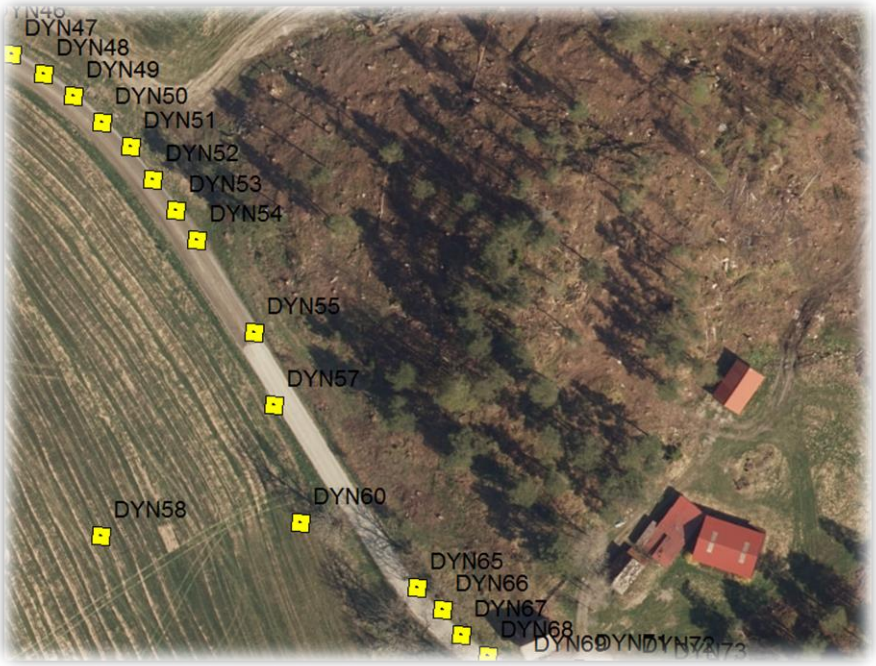

Figure 51 - A closer look at DYN55 to DYN 64

From point DYN55 to DYN64, only one point tracked its true position. The area to the right, shows a steep rocky hill blocking free sight to the east. It is likely that this is the cause of the bad positioning. *Figure 49* shows point DYN61-DYN64 heading north in a straight line ending up approximately 1750 meters off the route in DYN64. The fact that the points are in line, gives reason to believe that there are systematic errors causing the receiver to lose fix.

In the next part of the route (*Figure 52*) the ZED-F9P seems to able to retain fix, apart from DYN70 and DYN79 in between the houses and two minor rocky hills.

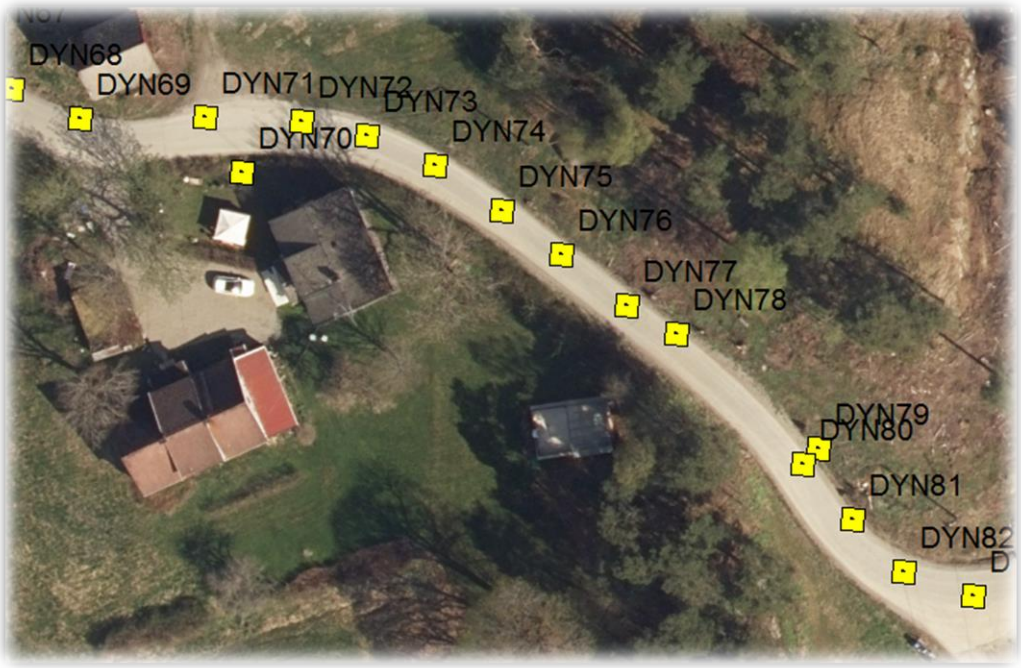

Figure 52 - DYN68 to DYN82

The last part of the route continues into a forested area, that starts off with losing and retaining fix several times. The final hundred meters, when the road is reaching a slightly elevated plateau with a clear view (except for the forest), the setup manages to keep the headlines of the route.

Figure 53 - DYN83 to DYN102

5.5 Precise Point Positioning

Table 33 shows the coordinate quality as calculated for the 1-hour measurements with the ZED-F9P, by the online PPP-service from Trimble. It is worth mentioning that these results are calculated using only GPS and GLONASS observations, which make the results less accurate due to the short time interval.

Table 33 - Coordinate quaility provided by CenterPoint RTX (Trimblertx.com, 2019)

Point ID	Receiver	Method	σ Lat.	σ Long.	σ Height
S1	u-blox 1h	PPP	0,019	0,046	0,028
S2	u-blox 1h	PPP	0,016	0,050	0,027
S3	u-blox 1h	PPP	0,039	0,040	0,035

6 Discussion

6.1 Static measurement

As *Point quality results* indicates, it is difficult to see clear differences between the coordinate quality from the measurements with the Leica GS16 and the ZED-F9P. The results show minor quality changes in favour of the Leica, but the differences might also be the result of random deviations.

Local conditions might affect the quality of the measurements. From a visual inspection, S1 is the point with the best prerequisites for measurements with high quality, because S1 have clear sight in most directions, whereas point S3 is closed in between two buildings with poor sight. Point S2 is located somewhere in between in terms of field of view. The resulting coordinate quality values does not show a clear pattern, which leads us to believe differences are more likely to be random deviations.

As for the length of the measurements, it is easier to see a trend in the accuracy. A shorter period gives in general higher values for the coordinate quality. In the following figures we have plotted the coordinate quality against the length of the measurements for receiver and benchmarks.

The plots show an increase for the 6- hour measurements with u-blox on all points, and on S3 with the Leica GS16. The reason for is not known. The measurements for u-blox on S1 and S2, are taken in the same timespan as Leica on the S3 on the 21st March. Temporal local circumstances could be an explanation, but this will not explain the increasement for S3 with the u-blox on the upcoming day.

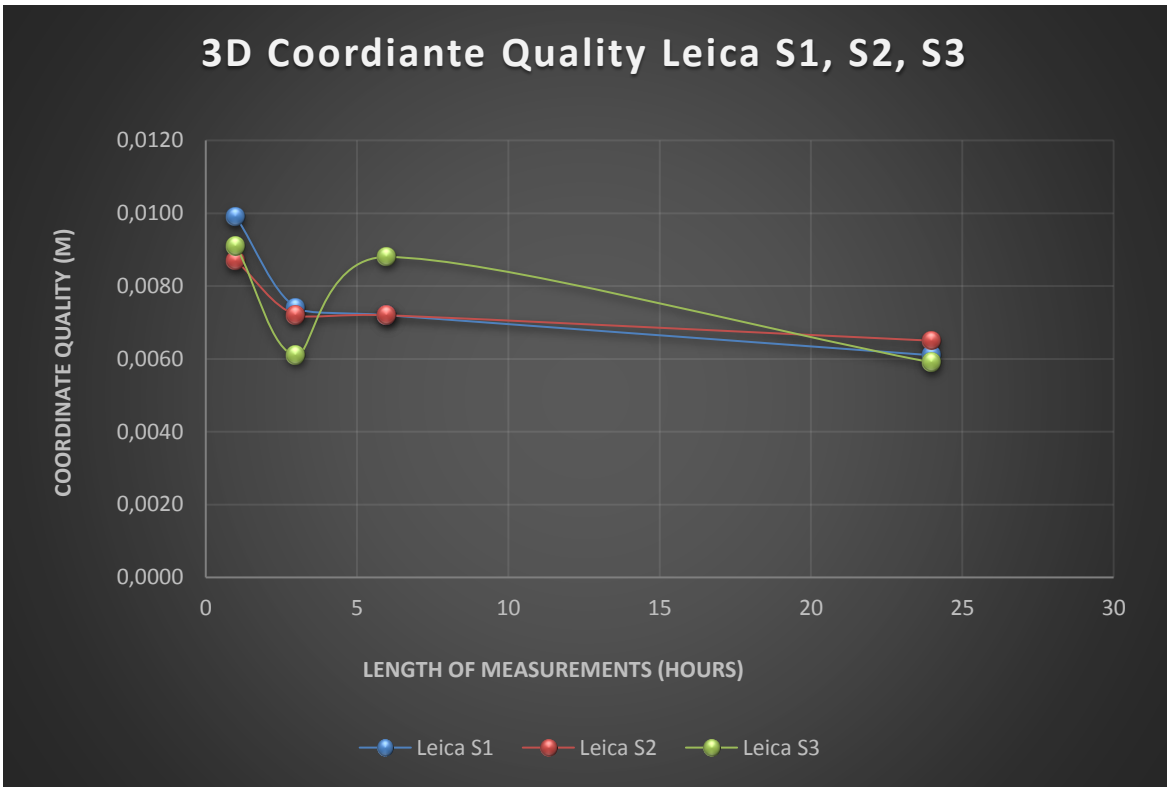

Figure 54 - Coordinate quality for Leica on S1, S2 and S3 against measurement time

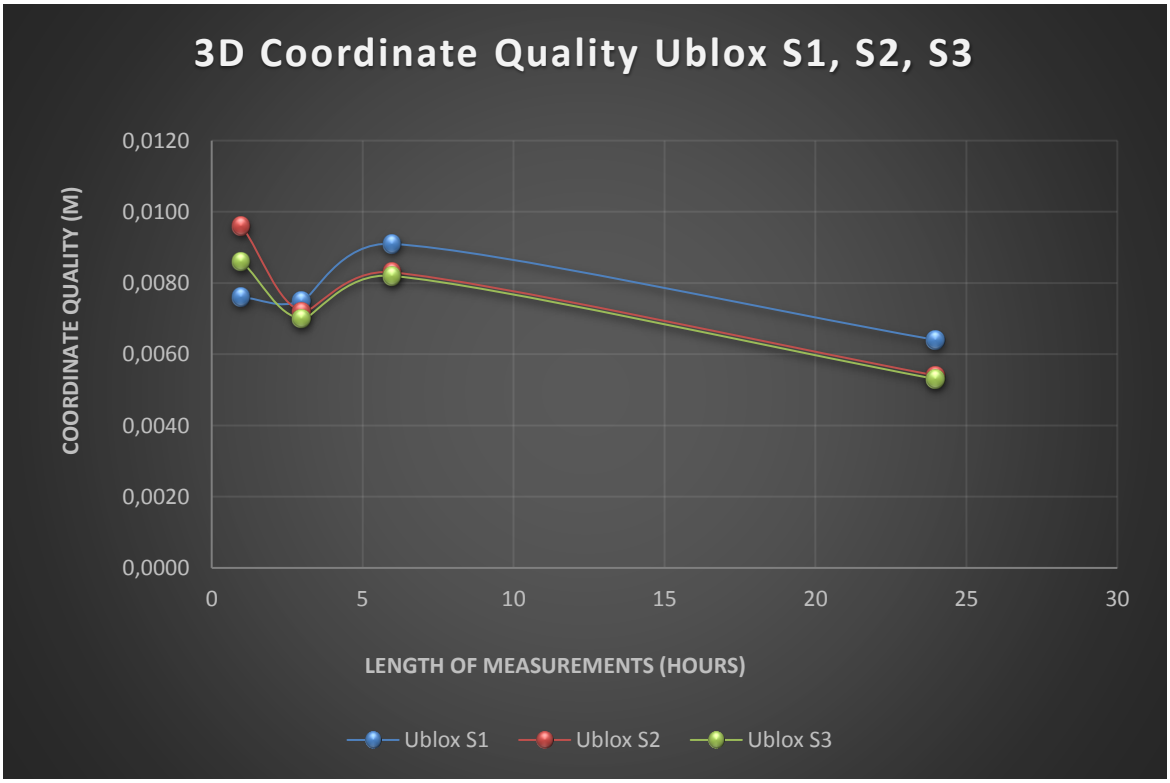

Figure 55 - Coordinate quality for ZED-F9P on S1, S2 and S3 against measurement time

The data supports our choice making 24-hour measurements as our foundation for the comparison. They have the best coordinate quality. The difference between the shorter measurements does not exceed 1-2 mm. The coordinate quality for the u-blox is in fact lower for two of the points. The calculated coordinates show that there had been problems with the height of S2, in the 24-hour measurements with the u-blox.

Based on this, we think the choice of using the 24-hour measurements with the Leica was a good choice. It is important to understand that in geomatics it is rarely possible to obtain absolute coordinates. It is about the probability of the calculated coordinates to be close to the absolute position. The necessity of measuring for 24 hours can be questioned. Considering the coordinate quality for 6-hour measurements only declines with less than 1 mm, the gain of measuring for 24 hours is miniscule. Even with the increased risk for irregularities, measuring for 3-4 hours might have been enough for our purpose and in future. This probably due to the excessive amount of satellites that are available now with four constellations compared with the two for just a few years ago.

The location of the phase center for the BT-152

As mentioned in *2.7.2 U-blox ZED-F9P*, no information was available on the location of the phase center of our antenna, which led to us calculating an estimate. From the previous figures, we have observed that the 24-hour measurements have the best quality. The heights measured with Leica for points S1, S2 and S3, spread with respectively 9.2 mm, 5.5 mm and 14.4 mm for all the measurements. For the u-blox these numbers are 8.5 mm, 14.1 and 10.2 mm.

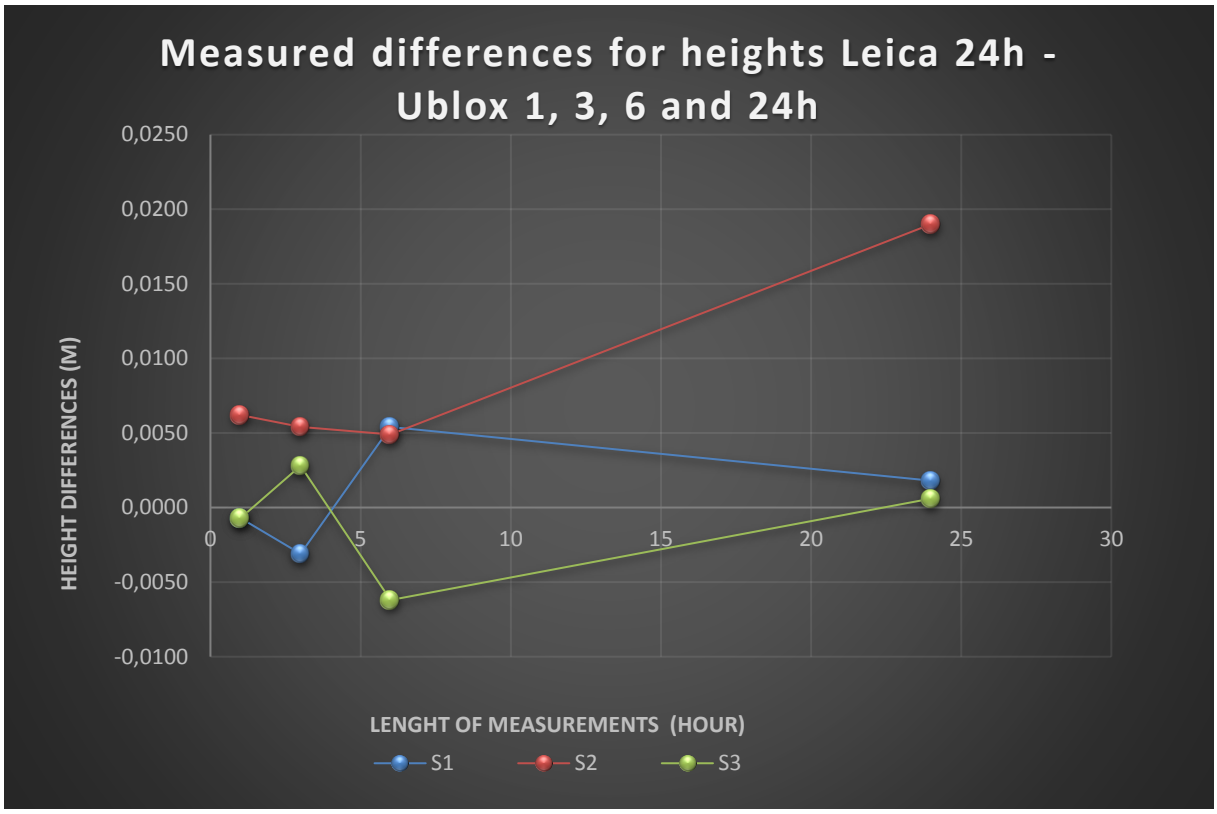

Figure 56 - Measured differences for heights between Leica 24h and u-blox 1,3,6 and 24 hours.

Figure 56 shows no clear pattern for the differences in measured heights between Leica 24h and the measurements with u-blox. The values for S1 and S3 are almost identical in the 0-line. The measured heights for S2, are approximately half a centimetre above. However, the values do not exceed the interval of all the measurements.

One exception is the 24-hour measurements, with the ZED-F9P being almost 2 cm off in height for S2, compared with Leica. This is unexpectedly high, especially because in the shorter measurements the difference is less than a centimeter; not only for S2, but also S1 and S3. It is likely that it is caused by unknown irregularities.

Stasjon	Dato/tid	3D KK [m]	ΔPos. [m]	Δhøyde [m]	ΔPos. og høyde [m]	y-koordinat [m]	x-koordinat [m]	Orto. høyde [m]
DOKK	03/12/2019 17:36:20	0.0002	0.0084	0.0045	0.0095	591,387.5140	6,740,432.9012	183.6063
SKRC	03/12/2019 17:36:20	0.0002	0.0023	-0.0012	0.0025	591,387.5068	6,740,432.8941	183.6119
MOEC	03/12/2019 17:36:20	0.0002	0.0029	-0.0047	0.0055	591,387.5079	6,740,432.8918	183.6155
LOTC	03/12/2019 17:36:20	0.0002	0.0060	0.0018	0.0062	591,387.5071	6,740,432.8888	183.6089

Figure 57- Calculated vectors between S2 and the base stations

Figure 57 shows the calculated vectors between S2 and the four base stations DOKK, LOTR, MOEC and SKRC. The calculated heights show a grouping within 1 cm. No vector is standing out. We have suspected snow as a possible cause to the problem, but this does not seem to be reflected by the coordinate quality of the given measurements. In fact, there is lower values for S2 than for the other measurements with the Leica GS16 on S1 and S3 that same day. Therefore, there is no reason to assume a connection with the phase center.

All in all, our qualified guess for the location of the phase center seems to be reasonable accurate. In order to perfect the phase center, we would either need more measurements, or a proper calibration of the antenna.

6.2 Real-time kinematic

With RTK measurements done by the u-blox setup, the main issue was software. As mentioned in *Planning*, the software used is made by the RTKLIB community, and has not been tested with the F9P prior to us testing it. Despite being untested, the software worked surprisingly well with RTK, with a few exceptions of the user interface freezing. RTKLIB is a good surveying tool. However, the software contains some limitations. One limitation, is that the software only is able to measure the point you are currently in. Other professional surveying software offer a range of other features, like displaying distances from a given point or line. The F9P is still a new product, so we certainly believe sure will be expanded functionality in either RTKLIB or another free surveying software in the near future.

6.2.1 Real time kinematic - Static

Every RTK static session consisted of 10 measurements with a cycle of two seconds. *Table 31*, shows the difference between the static RTK-measurements and the static 24-hours measurements by the Leica setup. S1 is the pillar which have the least obstacles in proximity, resulting in the highest accuracy in real-time of 5 mm in 2D and 15 mm in height. We considered S2 to be the pillar with 2nd most optimal conditions, but the GNSS-receiver struggles the most in this point. The reason might be due to a fence located nearby the pillar; the distance between fence and pillar is approximately 2.5 meter. The fence might work as a reflector for radio waves with the wave lengths used by GNSS-satellites. Investing in a higher quality antenna might eliminate those problems.

6.2.2 Real time kinematic - Dynamic

We chose to do a dynamic run in order to observe how the ZED-F9P would handle dynamic conditions. The measurements show that with free sight, the receiver manages to keep fix for every new position. The measurements do not show the accuracy, but in combination with the static RTK-measurements, show both high accuracy as well as high precision. Which makes it possible to assume that the ZED-F9P can handle dynamic measurements.

Based on both the static and the dynamic measurements, we believe that the weakest part of our setup is the antenna. We suspect that the antenna struggles with handling difficult situations where local conditions might cause the errors. This might be multipath or disturbances of the signals through vegetation or fences.

There are different thoughts of the required accuracy for lane level accuracy, but if we mind the 20 centimetres horizontally as a guiding value, we believe the ZED-F9P is capable of providing lane level accuracy (Report on road user needs and requirements, 2018). Due to being difficult to manually maintain a constant distance from the centreline of a road, lane level accuracy might be tested more accurately under controlled circumstances. On a minor scale this can be done with building guidance rails of wood to keep a trolley with the GNSS-receiver on a defined track. The exact position of the rails can be established with the help of a total station. However, it might be challenging on a bigger scale.

Another possibility is measuring on an unused railway track. Here it would be easier to make dynamic measurements over longer distances under controlled conditions, where the GNSS-receiver can be placed over one of the rails. This may make it possible to compare the measurements on the background of an orthophoto. The maximum point deviation is 35 cm for orthophotos, given by the Norwegian standard (Produktspesifikasjon for ortofoto i Norge, 2013), which specifies lower accuracy than the lane level positioning requirement. This means that the true position of the track needs to be confirmed by other measurements.

This is also a weak point we have seen in other tests, where receivers were tested on vehicles. With a required lane level accuracy of 20 cm or less, it becomes difficult to keep a constant distance to the centreline of the road.

6.3 Precise Point Positioning

As mentioned in *Planning*, the addition of online precise point positioning services is based around that it is free. Considering the price tag of the F9P, the targeted group for these services would be people that would like high accuracy points for personal use. This does not mean that PPP services cannot be used by professionals as well, but professionals would probably invest in a NTRIP service in order to achieve similar accuracy in real-time.

We encountered a small issue when using the PPP services, as they struggled to read all observations in the file we uploaded. This resulted in that only GPS and GLONASS observations were used to calculate the position, even though the file contained Galileo, BeiDou and even QZSS observations. The reason might be that the u-blox logs are converted to RINEX 3.03 which is not fully implemented by all services. Considering that we only submitted the 1-hour static measurement file, the coordinate quality of 5 centimetres is reasonable. On the other hand, if we were to process the same file manually in a software like Leica Infinity, with the use of reference stations, sub-centimetre accuracy is achievable.

7 Conclusion

7.1 Static

We were not able to see any major differences in coordinate-quality between the two GNSS-receivers as shown in chapter *5.3*. Except for the height in S2 for the 24 hour measurements, there is no clear pattern in the grouping as shown in chapter *5.3.5*. The patterns show typical random deviations. This gives reason to believe that the ZED-F9P is just as capable of static surveying tasks as the Leica GS16. Based on the outcome of further testing the antenna seems to be a limiting factor when it comes to multipath. We also experienced that logging for 24 hours is no longer viable. Although there are some small leaps in the graphs in chapter *6.1*, they show a tendency for the coordinate quality to flatten out after approximately 3-4 hours. As the results may indicate, RTKLIB did not have any issues with static measurements.

PPP gives anyone with a single GNSS-receiver the ability to achieve centimeter level accuracy. We found that most services providing PPP are not up to date. Nine out of ten services did not offer support for newer RINEX 3-formats. Trimble's service used in this thesis, did have support for newer formats. However, the service still failed to deliver a solution using all four constellations. Another issue with PPP services, is that there is not possible to get coordinates in a "custom" reference frame like EUREF89 with NN2000 heights without using software. This requires some knowledge of geodesy in order to get coordinates in any national reference frame. However, geographical coordinates might be enough in most cases. The results from the tables in chapter *4.3.2*, show that there is no difference in coordinates between the ones from the adjustment calculations in Leica Infinity, and Trimble's PPP-service, at least on a centimeter level due to lack of decimals. For heights, the differences ranged from 5 to 13 cm. Comparison of heights is often difficult due to different reference systems used as foundation for calculating heights.

7.2 Real time kinematic

Figure 47 is an example of our RTK observations and shows that the ZED-F9P can measure with high precision. Further, the RTK measurements have proven to achieve desired accuracy under optimal conditions with clear sky-view, similar to point S1. But the real time kinematic measurements have also given reason to believe that our antenna does not provide much resistance against multipath, since the accuracy in point S2 is lower than expected. Although point S3 is closed in by buildings, the fence near S2 seem to cause difficulties for the antenna. The module did not have problems with obtaining the fix-status. As for RTKLIB's functionality with RTK, there are limitations. Users are currently only able to save points, which restricts the amount of use-cases the F9P is viable. But when a larger amount of people become aware of the ZED-F9P, the functionality of freeware follows.

Testing in dynamic mode did not give the possibility to compare with benchmarks, but the layover of points on an orthophoto, gave an indication that under good conditions with free sight, the u-blox was able to provide reliable results. The receiver struggled with the rocky geology in the middle of the route, and the forested area near the end of the route. However, the u-blox managed to re-obtain fix-solution after reaching a plateau with better view of the sky. As mentioned above in the discussion of both static methods, it is likely that the antenna is the cause of the problems.

7.3 Recommendations

As for the future uses of the ZED-F9P, we have been slightly into autonomous vehicles and drones. Many types of drones come with a GNSS-module used for flight planning. The drone's route is pre-planned. Depending on the task, the georeferencing of the data is done with help from other sources, like ground control points. It is possible that in future, the GNSS-module might not only be used for flight planning, but also for collecting positional data with dynamic RTK. This in combination with an internal movement unit (IMU) registering the tilt of the drone in all directions (3D), might make it possible to reference data without the use of external sources. This spring, u-blox announced an update of the ZED-F9P; the ZED-F9K, which has a built-in IMU. U-blox is targeting the market for autonomous vehicles, but it would be interesting to see what it can do in a drone. And if it would be able to reference data directly with adequate accuracy, opposed the use of ground control points.

It is clear that GNSS alone will not be enough as guidance for autonomous vehicles. Therefore, u-blox provides the ZED-F9K with IMU-sensors. This will make it possible to calculate positions based on acceleration or deceleration in 3D. A necessity for being able to navigate in difficult conditions like towns, or as we experienced ourselves, heavy forested areas may be solved by an IMU. Even though IMU-based positioning might not be as accurate, it will make it easier for the GNSS-receiver to retain fix-status (for example after a tunnel). It would be interesting to see a comparison of calculated positions based on GNSS, against IMU-measurements, in order to see the differences in accuracy based on different parameters like distance, speed and surroundings.

A third interesting area for this new module, could be a combination with indoor positioning. There is an increasing need for accurate indoor positioning. Common for most of the systems, is the need for some form of beacons, radio waves, acoustic or IR. Indoor positioning is basically done in the same way as GNSS, and its predecessor LORAN, based on trilateration. The advantage of the use of an IMU for indoor positioning, is that it does not require any pre mounted equipment. And a combined GNSS-IMU will work 'everywhere'.

We have also seen that data format updates are presented by responsible bodies, but the implementation is rather unstructured. Services change format, but software manufacturers do not follow up, or vice versa. New satellite systems go global, but services still offer solutions

only based on GPS and GLONASS. This makes it difficult to use the advantages new developments and technologies offer. Affordable dual frequency receivers may become more common, and PPP services might become more willing to offer a wider variety of geographical reference frames. Rapid changes require rapid follow ups, also when is comes to services and software manufacturers

Erik Oppedal concluded for just a year ago, that receivers based on carrier phase measurements were too expensive. Now, one year later, we see that they have come within an affordable price range, which made it possible for us to analyse of the positional accuracy of a low-cost dual frequency GNSS-module.

References

Advanced Network Adjustment. (2017). 1st ed. [ebook] HeerBrugg: Leica Geosystems AG. Available at: https://leica-geosystems.com/-/media/80026c2d4e22481fb05a0df1fd2224f8.ashx [Accessed 10 May 2019].

aliexpress.com. (2019). *US $80.0 |Full frequency GNSS receiver Antenna GPS GALILEO GLONASS BEIDOU High Precision Survey RTK GNSS Antenna TNC connector, BT 152-in GPS Receiver & Antenna from Automobiles & Motorcycles on Aliexpress.com | Alibaba Group*. [online] Available at: https://www.aliexpress.com/item/Full-frequency-GNSS-receiver-Antenna-GPS-GALILEO-GLONASS-BEIDOU-High-Precision-Survey-RTK-GNSS-Antenna-TNC/32981828572.html?spm=2114.search0104.3.22.284177fcmxVqgf&ws_ab_test=searchweb0_0,searchweb201602_4_10065_10068_319_10059_10884_317_10887_10696_321_322_10084_453_10083_454_10103_10618_10307_537_536,searchweb201603_53,ppcSwitch_0&algo_expid=cc429afe-e676-40f5-81dd-a15bf9749eca-3&algo_pvid=cc429afe-e676-40f5-81dd-a15bf9749eca [Accessed 14 May 2019].

BBC News (2018). *How China's GPS 'rival' is plotting to go global*. [image] Available at: https://www.bbc.com/news/technology-45471959 [Accessed 26 Apr. 2019].

Bhatti, U. (2019). *Pseudo random codes*. [image] Available at: https://www.researchgate.net/figure/Pseudo-random-codes_fig7_306907130 [Accessed 13 May 2019].

Circuit Cellar. (2014). *Triangulation, Trilateration, or Multilateration?*. [online] Available at: http://circuitcellar.com/ee-tips/triangulation-trilateration-or-multilateration-ee-tip-125/ [Accessed 15 May 2019].

Coast Guard Aviation Association (2019). *LORAN chains established*. [image] Available at: https://cgaviationhistory.org/1959-loran-c-chains-established/ [Accessed 19 Apr. 2019].

Dale, J. (2018). *På rett sted til rett tid*. [ebook] Oslo: Regjeringen, pp.5,6. Available at: https://www.regjeringen.no/contentassets/abd1dec7647a4c22aaef7d93046e3f2b/pa-rett-sted-til-rett-tid.pdf [Accessed 26 Mar. 2019].

Difference Between GPS and DGPS. (2019). [Blog] *GrindGIS*. Available at: https://grindgis.com/blog/difference-between-gps-and-dgps [Accessed 18 May 2019].

En.beidou.gov.cn. (2019). *APPLICATIONS-Transport*. [online] Available at: http://en.beidou.gov.cn/WHATSNEWS/201812/t20181227_16837.html [Accessed 26 Mar. 2019].

En.wikipedia.org. (2019). *Global Positioning System*. [online] Available at: https://en.wikipedia.org/wiki/Global_Positioning_System [Accessed 10 Apr. 2019].

En.wikipedia.org. (2019). *Satellite navigation*. [online] Available at: https://en.wikipedia.org/wiki/Satellite_navigation [Accessed 4 Apr. 2019].

Encyclopædia Britannica Inc. (2019). *Frequency and wavelength*. [image] Available at: https://kids.britannica.com/students/assembly/view/223513 [Accessed 2 May 2019].

European Space Agency. (2019). *What is Galileo?*. [online] Available at: http://www.esa.int/Our_Activities/Navigation/Galileo/What_is_Galileo [Accessed 15 Apr. 2019].

Forssell, B. (2019). *Galileo – Store norske leksikon*. [online] Store norske leksikon. Available at: https://snl.no/Galileo [Accessed 4 Apr. 2019].

Forssell, B. (2019). *GLONASS – Store norske leksikon*. [online] Store norske leksikon. Available at: https://snl.no/GLONASS [Accessed 1 Apr. 2019].

Forssell, B. (2019). *GPS – Store norske leksikon*. [online] Store norske leksikon. Available at: https://snl.no/GPS [Accessed 23 Mar. 2019].

Galileognss.eu. (2018). *The path to high GNSS accuracy | GALILEO*. [online] Available at: https://galileognss.eu/the-path-to-high-gnss-accuracy/ [Accessed 6 Mar. 2019].

Gnssplanningonline.com. (2019). *Trimble GNSS Planning*. [online] Available at: http://www.gnssplanningonline.com/ [Accessed 4 Mar. 2019].

Gssc.esa.int. (2019). *Land Surveying - Navipedia*. [online] Available at: https://gssc.esa.int/navipedia/index.php/Land_Surveying [Accessed 10 May 2019].

Igs.org. (2019). *IGS News*. [online] Available at: http://www.igs.org/article/rinex-3.04-now-available [Accessed 11 May 2019].

Igs.org. (2019). *IGS Products*. [online] Available at: https://www.igs.org/products [Accessed 15 May 2019].

Kartverket. (2019). *CPOS*. [online] Available at: https://www.kartverket.no/posisjonstjenester/cpos/ [Accessed 18 Apr. 2019].

Leica GS16 Data Sheet. (2016). [ebook] Heerbrugg: Leica Geosystems, p.2. Available at: https://leica-geosystems.com/products/gnss-systems/smart-antennas/leica-viva-gs16 [Accessed 9 May 2019].

Leica Infinity brochure. (2019). 1st ed. [ebook] Heerbrugg: Leica Geosystems AG, pp.1,2. Available at: https://leica-geosystems.com/products/gnss-systems/software/leica-infinity [Accessed 5 Apr. 2019].

Leica Infinity. (2013). Heerbrugg: Leica Geosystems AG.

Mgex.igs.org. (2019). *IGS MGEX*. [online] Available at: http://mgex.igs.org/ [Accessed 9 May 2019].

Nischan, T. (2016). *GFZRNX - RINEX GNSS Data Conversion and Manipulation Toolbox (Version 1.05)*. [online] Dataservices.gfz-potsdam.de. Available at: http://dataservices.gfz-potsdam.de/panmetaworks/showshort.php?id=escidoc:1577894 [Accessed 4 Apr. 2019].

Norkart. (2019). *Oppmåling - Norkart*. [online] Available at: https://www.norkart.no/product/oppmaling/ [Accessed 11 May 2019].

NovAtel inc (2019). *Pinwheel OEM*. [image] Available at: https://www.novatel.com/products/gnss-antennas/oem-component-antennas/pinwheel-oem/ [Accessed 9 May 2019].

NovAtel. (2014). *Precise Point Positioning (PPP)*. [online] Available at: https://www.novatel.com/an-introduction-to-gnss/chapter-5-resolving-errors/precise-point-positioning-ppp/ [Accessed 15 May 2019].

Nptel.ac.in. (2019). *GPS Surveying Techniques*. [online] Available at: https://nptel.ac.in/courses/Webcourse-contents/IIT-KANPUR/ModernSurveyingTech/lecture4/4_3_Carrier_phase.htm [Accessed 6 May 2019].

Oppedal, E. (2018). *Analyse av posisjonsdata fra GNSS mottakere på kjøretøy*. [online] Trondheim: Eirik Oppedal, p.1. Available at: https://brage.bibsys.no/xmlui/bitstream/handle/11250/2561833/19123_FULLTEXT.pdf?sequence=1&isAllowed=y [Accessed 26 Mar. 2019].

Perkins, G. (2017). *Captivate Static GNSS settings*. [video] Available at: https://www.youtube.com/watch?v=zXZdzTf7hK0 [Accessed 26 Mar. 2019].

Price, J. (2019). *Dual-Frequency GNSS - An important location feature your phone is probably missing*. [online] xda-developers. Available at: https://www.xda-developers.com/dual-frequency-gnss-important-location-feature-your-phone-probably-missing/ [Accessed 13 Mar. 2019].

Product Summary U-center. (2019). [ebook] Ublox AG, p.1. Available at: https://www.u-blox.com/sites/default/files/u-center_ProductSummary_%28UBX-13003929%29.pdf [Accessed 13 Apr. 2019].

Produktspesifikasjon for ortofoto i Norge. (2013). [ebook] Hønefoss: Statens Kartverk, p.11. Available at: https://register.geonorge.no/data/documents/produktspesifikasjoner_Digitale%20ortofoto_v5_ortofoto-spesifikasjon-v4_5-2013_.pdf [Accessed 14 May 2019].

Report on road user needs and requirements. (2018). 1st ed. [ebook] Saint-Germain-en-Laye: European GNSS Agency, p.10. Available at: https://www.gsc-europa.eu/system/files/galileo_documents/Road-Report-on-User-Needs-and-Requirements-v1.0.pdf [Accessed 15 May 2019].

Rtklib.com. (2007). *RTKLIB: An Open Source Program Package for GNSS Positioning*. [online] Available at: http://www.rtklib.com/ [Accessed 5 May 2019].

Satelittbasert Posisjonsbestemmelse. (2009). 2nd ed. [ebook] Hønefoss: Statens Kartverk, pp.10,11. Available at: https://www.kartverket.no/globalassets/standard/bransjestandarder-utover-sosi/satbaspossystemer.pdf [Accessed 4 May 2019].

Sesolstorm.kartverket.no. (2019). *seSolstorm*. [online] Available at: http://sesolstorm.kartverket.no/ [Accessed 10 Apr. 2019].

Sesolstorm.kartverket.no. (2019). *seSolstorm*. [online] Available at: http://sesolstorm.kartverket.no/help.xhtml [Accessed 2 May 2019].

Shenzhen Beitian Communication Co. Ltd (2019). *AT-703 supported frequencies*. [image] Available at: https://www.aliexpress.com/item/Full-frequency-GNSS-receiver-Antenna-GPS-GALILEO-GLONASS-BEIDOU-High-Precision-Survey-RTK-GNSS-Antenna-TNC/32981828572.html?spm=2114.search0104.3.22.284177fcmxVqgf&ws_ab_test=searchweb0_0,searchweb201602_4_10065_10068_319_10059_10884_317_10887_10696_321_322_10084_453_10083_454_10103_10618_10307_537_536,searchweb201603_53,ppcSwitch_0&algo_expid=cc429afe-e676-40f5-81dd-a15bf9749eca-3&algo_pvid=cc429afe-e676-40f5-81dd-a15bf9749eca [Accessed 2 May 2019].

Skaar, J. and Linder, J. (2019). *lyshastighet – Store norske leksikon*. [online] Store norske leksikon. Available at: https://snl.no/lyshastighet [Accessed 4 May 2019].

Tersus-gnss.com. (2019). *Centimeter Precision Positioning GNSS RTK Technology*. [online] Available at: https://www.tersus-gnss.com/technology [Accessed 18 May 2019].

Trimblertx.com. (2019). *Trimble CenterPoint RTX Post-Processing Service*. [online] Available at: https://trimblertx.com/ [Accessed 12 May 2019].

ZED-F9P Data Sheet. (2019). [ebook] Thalwil: Ublox, pp.4-8. Available at: https://www.u-blox.com/sites/default/files/ZED-F9P_DataSheet_%28UBX-17051259%29.pdf [Accessed 9 May 2019].

Zucconi, A. (2017). *Positioning and Trilateration*. [image] Available at: https://www.alanzucconi.com/2017/03/13/positioning-and-trilateration [Accessed 12 May 2019].

Forssell, B. (2019). *Loran-C – Store norske leksikon*. [online] Store norske leksikon. Available at: https://snl.no/Loran-C [Accessed 19 May 2019].

Attachments

1. Point quality reports

2. Network adjustment reports

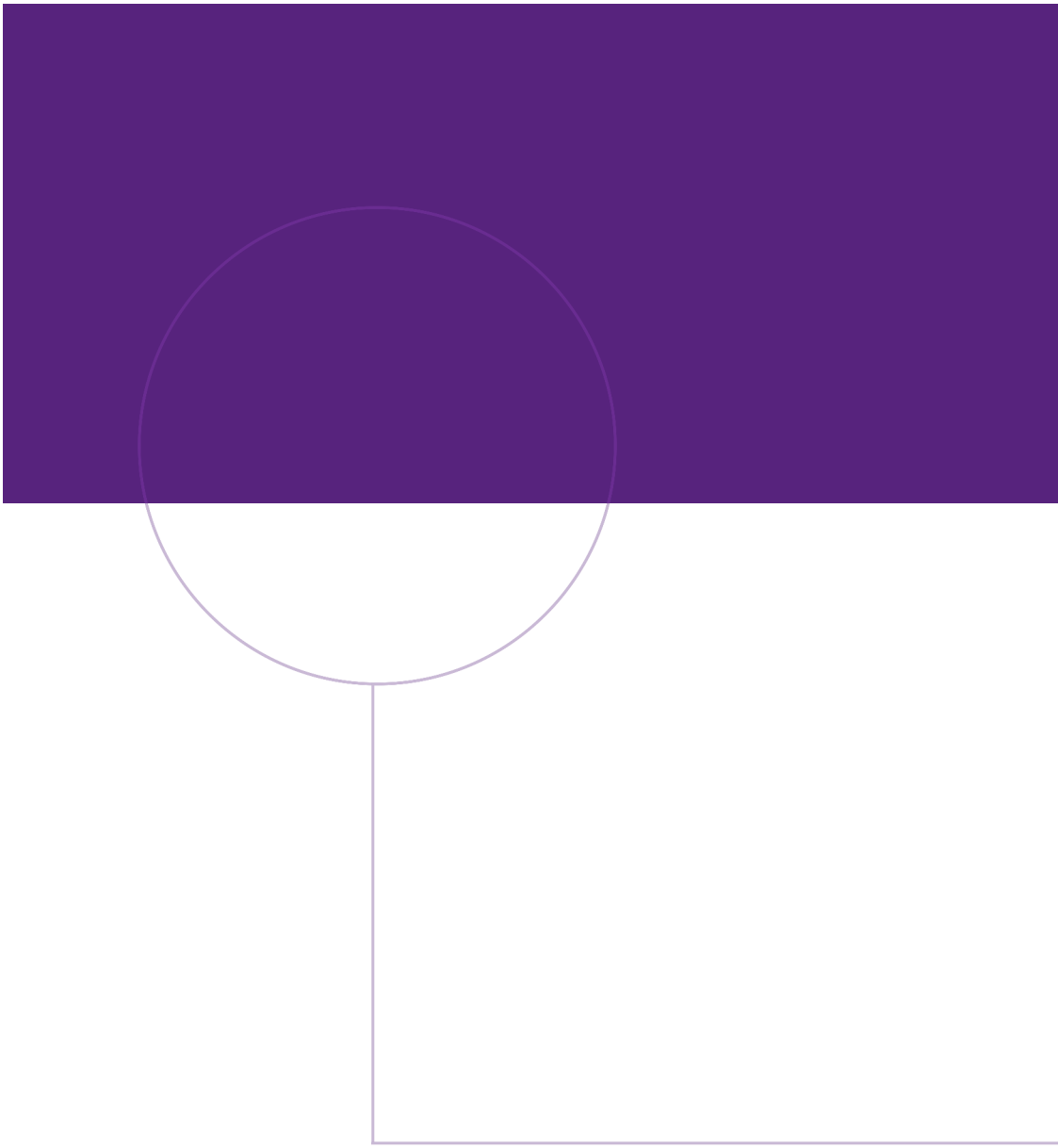

NTNU

Kunnskap for en bedre verden